Effect of Ag on Dielectric and Electrical Properties of Spinel Cobalt Ferrite

Name: Mehmood ur Rehman Khan

Reg. No: 00000119729

This thesis is submitted as a partial fulfillment of the requirements for the degree of MS in Materials and Surface Engineering

Supervisor Name: Dr. Iftikhar Hussain Gul

School of Chemical and Materials Engineering (SCME)

National University of Sciences and Technology (NUST),H-12

Islamabad, Pakistan

March, 2019

Abstract

In this study we took Co-precipitation chemical route to synthesize $CoFe_2O_4$ nanoparticles and loaded this with Silver one of the most electrically conductive materials as $Ag_xCo_{1-x}Fe_2O_4$ to study the effect occurred in its Electric and Dielectric properties in the presence of silver at different concentrations. XRD patterns confirmed the formation of pure $CoFe_2O_4$ and $Ag_xCo_{1-x}Fe_2O_4$ nanoparticles at x= 0.20, 0.35, 0.50 The average crystallite size found for pure $CoFe_2O_4$ nanoparticles was 31nm while for Silver loaded it is in the range from 34 to 44 nm. SEM shows uniformly distributed homogenous spherical nanoparticles grown by co-precipitation method. FTIR results confirmed the absorption peaks for $CoFe_2O_4$ and $Ag_xCo_{1-x}Fe_2O_4$ nanoparticles in the range 550-600 cm^{-1} and 380-450 cm^{-1}. Which confirms the presence of tetrahedral and octahedral sites in spinel ferrite structure. The dielectric parameters were studied and dielectric constant (ε'), dielectric loss (ε"), dielectric loss tangent (tan δ) decreases with increase in frequency and increases with increase in concentration x of silver in $CoFe_2O_4$ and these properties enhanced promisingly. Impedance decrease with increase of concentration of conductive metal silver offering more electrons to move between the cations. The A.C conductivity is maximum at higher frequency which represent the dominance of hoping conductivity over band conductivity. The electric modulus increases with increase in frequency and decreases with increase in concentrations of silver in $CoFe_2O_4$. The Cole-Cole plot of electric modulus gives semi circles curves and relaxation time at higher frequencies. The resistivity "lnρ" of the prepared samples was plotted against "$1/k_BT$". A decrease in DC electrical resistivity with increase in temperature has been observed. These variations in the Electric and Dielectric properties of $CoFe_2O_4$ due to silver made it an important material for the electromagnetic devices and biomedical applications.

Table of Contents

List of Figures

List of Tables

Chapter 1

Introduction

1.1 Ferrite

A kind of ceramic materials composed from Iron oxide (Fe_2O_3) tied with some other metal elements also Oxide materials containing ferric ion (Fe^{3+}) as principal constituents are known as ferrites [1].

They are dark grey or black in appearance having hard, brittle and polycrystalline properties along with magnetic properties. In general Ferrites from magnetic point of view they are ferrimagnetic ceramic materials in nature due to presence of ferrimagnetic oxides with larger portion of ferric and metal oxides in it [2]. These ferrimagnetic materials don't have moment alignment but different and distinguishable arrangements of magnetic moments which includes perpendicular and parallel moments, effect of this kind of arrangements give them unique and interesting properties and it is result of many different structures of crystals. Due to this every different ferrite offers different diverse applications, it all depends on crystal structure order. Ferrites possess very high electrical resistivity, due to these high values of resistivity they have capability to limit the generation of eddy currents so we say they limit eddy current loss. Due to these they are also called insulating materials [3]. These ferrite materials also possess medium permittivity, greater saturation magnetization and permeability. If they face too much high heat, they even lose their magnetism. With these above-mentioned wide range of properties and ability to have different properties with varying mixture of iron oxide and other materials gives us opportunity to tailor and get electrical and magnetic properties according to our desire and need [1]. we find no other materials around [4], making them unique magnetic materials and this gives them applicable tendency in approximately all fields. First ever time in the history Magnetic north was located by using magnetic iron oxide [5].

1.2 Brief History of Ferrites

In the history Ferrites have been known to mankind from multiple centuries, they are using them in different ways to ease their daily work even if they don't have direct

knowledge about the but it is evident, they were familiar with the properties and effect of ferrites from early ages. The word “Ferrite” originated from Latin language word “ferrum” which means or used for “Iron” and iron is important component of ferrites or simply magnetic oxides. The description of one of the ancient known ferrites found in about 800 B.C Greek writings is “loadstone” also known as magnetite (Fe_3O_4) which attracts iron and is naturally occurring nonmetallic solid. other early people were also familiar with it as term Magnetism came to knowledge which is important property of ferrites, this word was derived from “Magnesia” [5]. Chinese also knew about properties of loadstone and utilize it in compasses for navigation purposes to locate magnetic north of earth. For the first time in the history magnetic north was located by using magnetic iron oxide loadstone which made it clear on people that earth itself was a magnet and needle of compass which was made magnetic by rubbing it with loadstone always point towards the magnetic north of the earth. And this whole thing was in 1600 first ever scientific study on magnetism known as “De Magnate” which was published by physicist William Gilbert. Then in 1819 Scientist with the name Christian Oersted noticed the deflection in needle of magnetic compass when brought near to the electric current carrying wire which led to the discovery of electro magnets in 1825 [5]. In the year 1930 the scientific and practical study of structural, magnetic and electrical properties of ferrites, their use and applications were started, form then many researchers broadly done the study on them.

1.3 Types of Ferrites

Ferrites are classified in two main categories on the basis their magnetic behavior or hysteresis loss and Structure. Types of ferrites on the basis of magnetic behavior or simply hysteresis loss includes Soft ferrites and Hard ferrites [3]. While kind of ferrites on the basis of structure includes Spinel ferrites, Garnets and third one is Hexagonal ferrites [1]. First of all, brief description of soft and hard ferrites is as following.

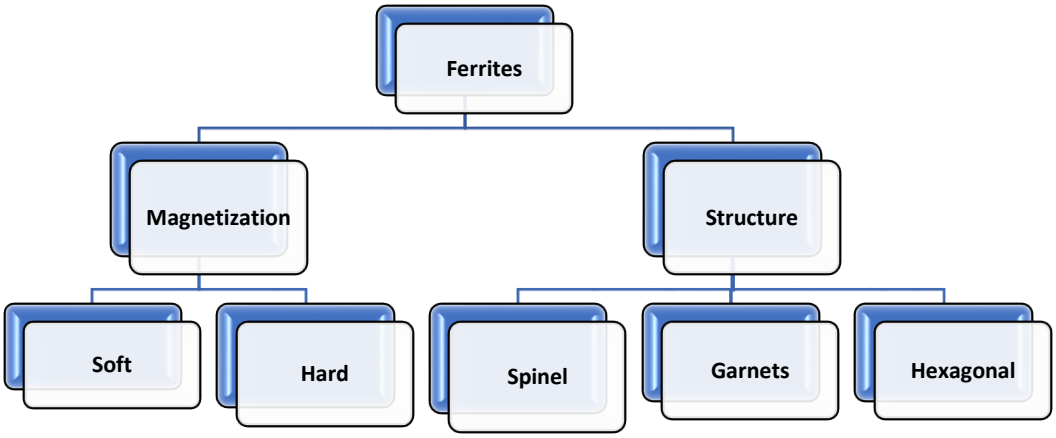

Figure 1.1 Classification of ferrites on the basis of structure and magnetization

1.3.1 Soft Ferrites

These ferrites in the presence of magnetic field magnetize and de magnetize very easily which means they have very low energy dissipation in magnetization and de magnetization along with low coercivity [2]. In other properties of soft ferrites, their permeability is low where they have low coercivity their coercivity is always less than 1000 A/m and they have narrow hysteresis loop so we say low saturation magnetization, low magnetostriction and Curie temperature is also low [3]. They also bear very high values of resistivity so They prevent the energy losses in transformer cores and inductors etc. They appear dark black or gray also very hard and brittle. Soft ferrites are used in many applications, power electronics circuits, inductors, small size antennas, chocks, volatile and nonvolatile memories etc. are some useful applications of soft ferrites [4]. Ferrites like $MnZnFe_2O_4$ and $NiZnFe_2O_4$ are the two examples of soft ferrites.

1.3.2 Hard Ferrites

ferrites which in the presence of magnetic field do not magnetize and de magnetize easily and take large time for this purpose having wide hysteresis loop called Hard ferrites [1]. They have the high value of coercivity, high remanence, high saturation magnetization, high magnetostriction, high permeability and high Curie temperature (Tc) which make them permanent magnets. These materials are also known as ceramic magnets [2]. They are very cheap in cost because of the easily availability of the raw

materials to make them. Due to this they are widely used house hold appliances cars, electrical devices also used for purpose of high-density storage and in audio and video tapes. Some of the important hard ferrites are $BaFe_{12}O_{19}$, $SrFe_{12}O_{19}$ and $CoFe_2O_4$.

These applications of hard and soft ferrites and their low costs make ferrites very useful candidate in the innovative applications [3].

Table 1.1.1 Comparison between Hard and soft ferrite

Comparison				
	Hard Ferrite		**Soft ferrite**	
	High	**Low**	**High**	**Low**
Saturation Magnetization	✓			✓
Coercivity (Hc)	✓			✓
Permeability	✓			✓
Remanence	✓			✓
Magnetostriction	✓			✓
Curie temperature (Tc)	✓			✓

Now a brief description of categories which ferrites have on the basis of structure which are as followings.

1.3.3 Spinel Ferrites

This type of ferrites which are called Spinel ferrites are the subtypes of Cubic Ferrites. The structure for the spinal ferrites known as spinal structure is first discovered by Braggs and Nishikawa in 1915 [6]. "MFe_2O_4" is a general formula used for spinel ferrites, where M is a divalent cation. Some examples of divalent cations include copper (Cu^{2+}), cobalt (Co^{2+}), zinc (Zn^{2+}) and nickel (Ni^{2+}). Spinel ferrites have the simple structure as compared to the other ferrite types [7]. The spinel structure is close packed face centered cubic (FCC) structure. Its unit cell is composed of 32 Oxygen

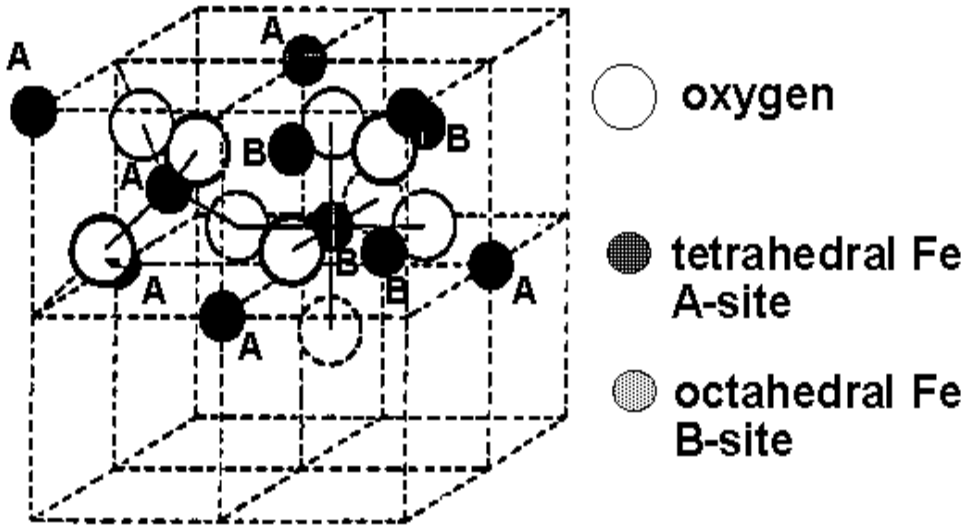

Figure 1.2 Spinel ferrite unit cell with octahedral and tetrahedral site [56]

ions [1]. There are two types of as Tetrahedral denoted by A second one is Octahedral denoted by B as also in fig 1.2. The (A) site is surrounded by 4 oxygen atoms [7]. There are 64 tetrahedral sites in spinal ferrite structure out of which 8 tetrahedral sites are occupied by cations. The (B) site is surrounded by 6 oxygen atoms. There are 32 octahedral sites in spinal ferrite structure out of which 16 octahedral sites are occupied by anions. The occupation of the A and B sites result into the electrically neutral structure of spinal ferrite. Their high value of electrical resistivity and low eddy current are those properties which made the spinal ferrites the most broadly used family of ferrites. They have very excellent electrical and magnetic properties [6]. The spinal ferrites are further classified on the basis of their cations distribution on tetrahedral and octahedral sites [7]. They are classified in the following groups.

- Normal Spinal Ferrites
- Inverse Spinal Ferrites
- Mixed Spinal Ferrites

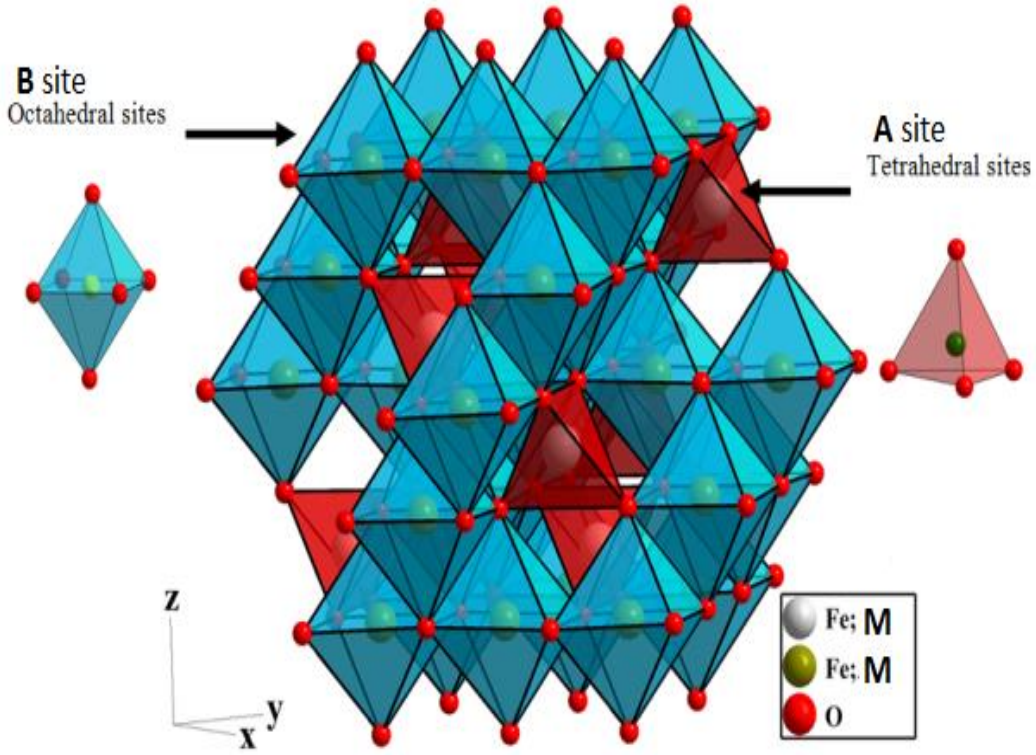

Figure 1.3 3D model of Octahedral and tetrahedral sites in unit cell [8]

This whole document or discussion surrounds about spinel ferrites, to develop complete picture and understanding about the spinel ferrites we must have complete insight of these ferrites. For this purpose, we now briefly take a look at above mentioned three types of Spinel ferrites which are as following.

1.3.3.1 Normal Spinel Ferrite

Spinal Ferrites are normally composed of trivalent and divalent ions. Those ferrites in which within crystal structure, B sites or octahedral are occupied by the trivalent metal ions. On the other hand, A sites or we say Tetrahedral are occupied by divalent metal ions are called normal spinel ferrites [7].

1.3.3.2 Inverse Spinel ferrites

Within the inverse spinel structure both the tetrahedral sites (A) and octahedral sites (B) are occupied partial by the trivalent metal ions remaining divalent ions distribute themselves randomly on B sites [7].

1.3.3.3 Mixed Spinel ferrites

In the third type of spinal ferrites which is “Mixed Spinal Ferrites” both octahedral and tetrahedral sites are occupied by trivalent and divalent ions both. In case of mixed spinal ferrites, the number of trivalent and divalent ions on octahedral sites are unequal

unlike inverse spinal ferrites in which half of the octahedral sited are filled by divalent ions and half by trivalent ions [7].

Table 1.1.2 Types of spinel ferrites, Summary

Types of spinel structures	
Normal spinel	**A site occupied by metal cations and B site by Fe^{3+} cations.**
Inverse spinel	**A site completely occupied by Fe^{3+} cations and B site randomly by both Metal cation and Fe^{3+}.**
Mixed spinel	**Both sites occupied by cations intermediately**

1.3.4 Garnet Ferrites

These ferrites were discovered by Giller and Gilleo in 1957. The general formula of such ferrite is $M_3Fe_5O_{12}$, where M is the rare-earth trivalent ions. Some rare earth trivalent ions are Gd, Dy and Y etc. They have cubic structures and are magnetically hard materials [3].

1.3.5 Hexagonal Ferrites

The general formula of hexagonal ferrite is $MFe_{12}O_{19}$ or also $6Fe_2O_3 – 1MeO$, where M can be barium, cobalt strontium or combination of these. Its structure is similar to spinel structure. There are 3 sites in such ferrite which are tetrahedral, octahedral and tri-gonal sites in which metal ions are occupied. Their hexagonal structure consists of two types of oxygen layers. The first layer is made of four oxygen ions where the second layer is made of three oxygen ions and the fourth site in this layer is occupied by barium ion [3]. Besides these two layers there are also tetrahedral, octahedral and trigonal bipyramidal interstitial sites between the layers which are surrounded by four, six and five oxygen ions respectively [8]. Due to their high values of coercivity they got a lot of attention in practical applications. These materials are very important in

the field of electronics and telecommunications, they are widely used in loud speakers, microwave applications, magnetic recording devices and as fridge magnets [5].

1.4 Cobalt Ferrite ($CoFe_2O_4$)

Cobalt ferrite is a very important material. It has captured the attention of the researchers due to so many useful applications in magnetic fluids, magnetic recording devices, high resistivity and many more [5]. Cobalt ferrite ($CoFe_2O_4$) has good chemical stability and excellent mechanical hardness. Cobalt ferrites are the cubic ferrites. These have the inverse spinal structure. Where Fe^{3+} is located at A and B sites and Co^{2+} is located at B site [4]. Cobalt ferrite has the anisotropy constant value in the range from 1.8 to 3 x 10^6 erg/cm^3. The use of the cobalt ferrite in the magnetic recording devices must possess the high value of coercivity. High value of coercivity depends on the particle size of the material. The particle size near the critical size of the particle has the larger value of coercivity. The critical size is equal to the size of single domain. Co-precipitation and sol gel processes are widely used for the synthesis of cobalt ferrite nanoparticles [9]. Fe (III) and Fe (II) salts are used for the synthesis of the cobalt ferrite nanoparticles. The electrical, dielectric properties of the cobalt ferrite are of great concern. There are so many applications related to the electrical and dielectric properties of the ferrites [10]. A lot of work has been done on these properties. Dielectric constant, dielectric loss, ac and dc electrical resistivity are very dependent on the crystal structure, grain size of the cobalt ferrite [11]. The crystal structure and grain size is depends on the process by which the material is formed. AC conductivity (σac) increases by increasing the frequency. The dielectric loss is due to the imperfection and impurities in the crystal lattice. Dielectric constant (ε′) also changes on changing the frequency [12]. The reason for the change in dielectric constant with the frequency is that the ferrites conversion from ferromagnetic to paramagnetic on changing the frequencies. The dielectric constant (ε′) also changes with changing the temperature.

1.5 Silver (Ag)

It is also one of the very important from the history of mankind as the benefits of this metal were known to mankind from the very beginning. The main reason for this is that it is easily available in uncombined form in earth and mined out of it in central and south America, Peru, Germany etc. Humans are using as currency from ancient

times back to Romans and Greeks along with the Gold. It is Soft, shiny metallic look and it tarnish very quickly in air as it is reactive to sulfur present in the atmosphere.it was also used as Jewelry is also very good conductor of electricity even higher than the copper which make it useful for electronic or electrical purposes making electrical contacts. The paint of the silver is utilized in producing printed circuit boards. Due to its property of high reflection it is used to make mirror and find great application in the field of physical Optics. Because of its sensitivity to visible light it is made to use in photography, light sensitive glass of lenses. It also bears great antibacterial properties which make its role in medical industry wide, Silver Nano particle are used in clothing against bacteria. It also has wide range of application in electronics industry.

1.6 Nanoscience

NANO is the science of today, it tightens it grip on all over the world. It consists of several disciplines of science like, Physics, Chemistry, Biology, material science etc. It has a lot of applications which are available in markets now days. Nanomaterials have totally different properties than bulk materials. The physical properties of a substance changes as we move from its bulk form to its Nano form. We can define Nano-materials as, those materials which have structured components with at least one dimension less than 100 nm. On the basis of dimension structure, the Nanomaterial are categorized as 1-D, 2-D and 3-D. 1-D are those Nanomaterials whose one dimension is constrained only, examples of 1-D Nanomaterials are thin films and surface coatings [13]. Its sizes can be varying in 2-dimensions, while its 3rd dimension will always have constrained less than 100nm. Similarly, in case of 2-D and 3-D Nanomaterials 2 and 3 dimensions will remain less than 100nm in its Nanoscale materials. For example, Nanotubes and Nanowires are 2-D Nanoscale materials in which two dimensions are always remain in the range of Nanoscale. Precipitates, collides and quantum dots are the examples of 3-D nanostructures. In case of these particles, all the three dimensions are constrained to nanoscale. Which means that all the three dimensions of a 3-D nanostructured material remain less than 100 nm.

As the nanomaterials have different properties than its bulk counterpart. The main reasons which are responsible for their changes in properties on nanoscale are relatively large surface area and quantum effect [13]. These two reasons or properties of a material are responsible for the change of different material properties like

electrical properties, strength and their reactivity. As we move from bulk to nanoscale, surface to volume ratio of a material increases which in the result enhances different properties like electrical properties and magnetic properties. We can tailor and control properties of a nanoscale material by controlling or tailoring its particle size [14].

In nanotechnology or Science, a new material is fabricated rather by handling different and new techniques (like a vast variety of techniques used for the fabrication of thin films) or in the result of self-assembly. Nanotechnology has already been given us a lot of new materials and new methods in almost all fields of science and yet more to be discovered. Those materials are very important and useful in those fields.

1.7 Dielectric Properties

Ferrites have high activation energy which indicates their high resistivity at room temperature. This property of ferrites makes them suitable for applications as dielectric materials. The non-conducting materials are mainly used as dielectric materials, it is very informative to study the interaction of electric field with the atoms of dielectric materials. In dielectric materials polarization occurs when they are exposed to an electric field, the polarization results due to the occurrence of induced dipole moments. When an electric field is applied the electron, cloud move to one side resulting in the creation of dipoles which is characterized by its dipole moments [5]. In dielectric material each atom creates its small field, and this field interact with the field which is applied from the outside [15]. That process in which the negative charged electron cloud and positive ions of atoms or molecules are separated and then the dipole is oriented accordingly to the applied field or the separation of charge carriers which occurs at the interfaces of grain-boundaries in the result of applied electric field is known as electric polarization [10].

Polarization is categorized in the following main four types.

•Electronic polarization

• Ionic or atomic polarization

• Dipolar polarization

• Interfacial or space-charge polarization

The electric polarization is referred to interfacial or space-charge polarization as it is related with the trapped and mobile charges. This type of polarization mainly occurs in the amorphous and polycrystalline materials because in such type of material charge

carrier like electrons, holes and ions are trapped on some sites and they get mobilize after getting some energy [16] . The mechanism which is responsible for the transportation is defined by knowing the dielectric behavior of a dielectric material depends upon of a dielectric material is its dielectric material depends upon which generally defines dielectric material depends upon a dielectric material. The dielectric constant of a dielectric material depends upon the following factors. Frequency of alternating electric field, Rate of change of time-varying field, Chemical structure of dielectric material, Imperfection (defects) of the material, Physical parameters like pressure temperature etc.

The dielectric constant and the dielectric polarization field both depends on each other. The dielectric polarization fluctuates accordingly to the fluctuation of external field, but there is always a lag between them. If the fluctuations of dielectric polarization do not follow the fluctuations of external field then the dielectric of that material decreases [17]. In case of low frequency applied fields, the polarization follows the fluctuations of the field and hence in that case the dielectric constant remains almost constant. In case of high frequency applied fields, the polarization cannot follow the field and its dielectric constant decreases and at one stage when the frequency to very high value then the orientation polarization stops due to relaxation of dielectric materials [18]. There are different limits of frequencies at which the different types of polarization (ionic, electronic etc.) stops.

1.8 DC Electrical Properties

There are three basic types of materials which are conductors (metals), insulators and semiconductors [2]. They are categorized on the basis of their tendency to carry electric charge. The materials which are good carrier of electric charges i.e. having higher conductivity have the lower activation energy. The insulators have very high activation energy. In case of some insulators and semiconductors their conductivity increases by increasing temperature but in case of metal a gradual decrease occurs in the conductivity of metals as we increase the temperature. Ferrites are structure sensitive materials the conduction of electric charges in the ferrites depends upon the structure of the ferrites. The structure of ferrites can be changed by its synthesis route, amount of substituents, annealing temperature, reaction temperature, type of substituents etc. [2] As compared to metals, ferrites have high electrical resistance and

its electrical resistivity can be controlled or enhanced by the controlling the factors defined above [19].

By the electrical properties of a materials depends on the generation of the electric charges in the material and their transport inside the material. In ferrites the conduction or transport of charge carriers occur in the form of hopping which is explained in the Verwey model [20]. The hoping of charge carriers in the ferrites occur between the ions at sites octahedral. The jumping on the separation from one to other the ions, for the conduction of charge in ferrites the charge carries must have overcome the potential barriers i.e. the charge carrier should have much energy to hope from one ion to another. That minimum energy which charge carrier required to overcome the potential barriers is known as activation energy [21]. The transportation of charge carriers in M-type ferrite materials is also occurred by hopping thus they are hopping semiconductors or it is said to be small polar an hopping semiconductors having large number of mobile electrons [22]. The hopping of electrons ferrites occurs between the Fe^{3+} and Fe^{2+} ions which are situated on octahedral sites [21]. This exchange can be different in different materials depending upon the orbital overlapping of Fe^{3+} and Fe^{2+} with oxygen [23].

1.9 Magnetism

The term “magnetism” was derived from the word “magnesia”, which is an island of Aegean Sea where the certain types of stones were found back in 470BC which attracts iron and were named as lodestones [1]. The history of magnetism is very old but its understanding began in twentieth century. Chinese employed magnets in various navigation applications such as compass in the 12 century [5]. A famous physicist William Gilbert manufactured some artificial magnets and proved that the compass will always point towards north-south because earth itself has a magnetic property. In 1750, John Michel showed that the magnetic poles will always obey the inverse square law which was later proved by Charles Coulomb. The first electromagnet was manufactured in 1825 when the fact was discovered that magnetic field is produced by an electric current. Faraday, Becquerel and Bergmann later discussed the effect of magnetism on liquids and gases and found out some of them has a noticeable extent [5]. The whole concept of magnetism revolves around the dipole and magnetic field. The magnetic field shows the volume of space in which change in energy occurs which can be detected and measured. Whereas magnetic poles describe the location of where

the magnetic field is detected to be entering and leaving within the magnetic material. Magnetic poles do not exist in isolation rather they occur in two opposite poles (North and South Pole) which are separated by a distance and forming a dipole. The North-Pole describes that the magnetic field is leaving the dipole and South-Pole describes that the magnetic field is entering the dipole. By cutting the magnet bar into pieces; two or more dipoles or magnets can be created. The response of the material when it is subjected into magnetic field is called magnetism. Some materials response attracted behavior, some response repelled behavior and some response unaffected behavior when they are subjected to applied magnetic field. The magnetic response disappeared after a critical temperature which was studied by Curie; he examined that magnetic materials response no magnetic behavior after a certain temperature which is termed as Curie temperature [3]. Every material has its own Curie temperature for which it shows no magnetic response.

Anything which has weight and occupied space is called matter which is composed of atoms. The atoms constitute on protons, neutrons and electrons. The electrons revolve around the nucleus with constant motion and also revolve round its own axis whereas the protons and neutrons are present in the nucleus of atom. Hence electrical charge is in motion then a magnetic field is produced in an atom [24]. One is the motion of electron around the nucleus of an atom which is similar to the rotation of planets around the sun in our solar system. The second is the spin of electrons round its own axis which is similar to the Earth's rotation round its own axis. The electrical charge is in motion then a magnetic field is produced, whereas electrons have negative electrical charge which takes part in producing magnetic field. When an electrical charge is in motion then a magnetic field is produced. Pauli Exclusion Principle shows that for large fraction of elements the magnetic moment of electrons will cancel each other. electrical charge is in motion then a magnetic field is produced of magnet which determines he torque it will experience when an external field is applied [5]. Pauli electrical charge is in motion then a magnetic field is produced of opposite spin can be occupied in each electronic orbit. A certain number of transition metals do not cancel magnetic moment i.e. iron, nickel and cobalt; such elements are the examples of magnetic materials. Magnetic moment arises in such transition metals from the spin of electrons. But there are also certain numbers of elements which do not cancel orbital motion of electrons and show magnetic behavior; such elements are rare earth metals

i.e. europium, neodymium, samarium and cerium [2]. Besides of these rare earth metals and transition metals, magnetism is also observed in a variety of chemical compounds which contain these elements. Metal oxides are the examples of such chemical compounds in which oxygen is bonded with metals.

1.10 Types of magnetism

If a material is placed in a magnetic field then it shows various kinds of behaviors depending upon the various factors like the net magnetic moments of atoms or the atomic and molecular level of structures. As we know that magnetic moment is associated with the orbital and spin motion of electrons, which can be alter by the applied external field. With applied external field, some materials align themselves parallel to it while some materials align themselves opposite to it. Electrons are usually found in pairs in an atom which spin in opposite directions, that's how magnetic field is cancelled [2]. Those materials that have unpaired electrons show some net magnetic field. Based on these characteristics, the magnetic behavior can be classified as in Figure

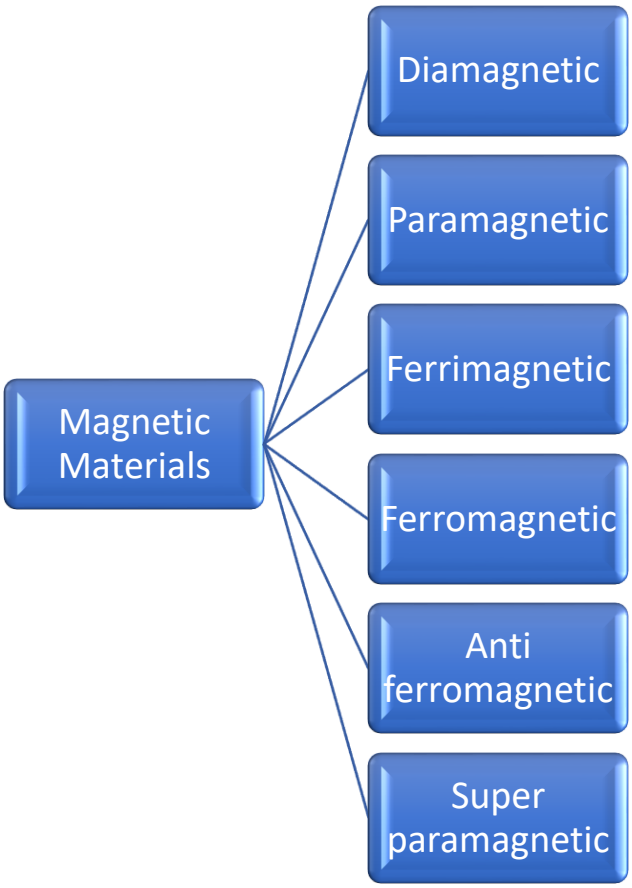

Figure 1.4 Types of magnetic materials

1.10.1 Diamagnetism

In diamagnetic materials, the magnetic moment is zero and thus has no internal magnetic interactions. In such type of materials, the external shells of their atoms are completely occupied. When diamagnetic materials are placed in the external magnetic field, the orbiting electrons are disturbed because of change occurs in its orbital angular momentum. The change in orbital angular momentum induces a magnetic moment in the diamagnetic material which always opposes the external applied magnetic field thus diamagnetic materials are opposes by external magnetic fields and thus having a negative susceptibility. Materials with filled shells and having even atomic number like N_2, He, H_2 and compounds like NaCl show diamagnetic properties [2].

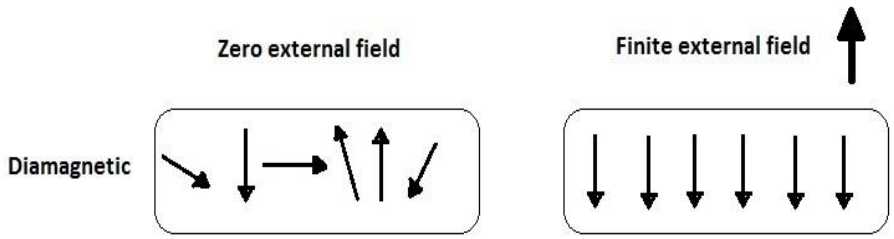

Figure 1.5 Atomic dipole configuration of diamagnetic material [7]

1.10.2 Para magnetism

Paramagnetic materials show magnetization only in the presence of external magnetic field. Paramagnetic materials consist of permanent dipoles which are randomly oriented inside the magnetic materials in the absence of external magnetic field. The dipoles are arranged randomly canceling the magnetic effect of each other and shows a zero-net magnetic effect on the material. When a paramagnetic material is placed in an external field, a torque is provided to the magnetic dipoles and they align themselves in a proper direction i.e. in parallel or in anti-parallel direction to the applied magnetic field and they get magnetized. But when the external magnetic field is removed then the aligned dipoles again loss their energy in no time and go back to their original random positions and shows no magnetic properties again. Paramagnetic materials have positive susceptibility because they are attracted towards the source

which applied an external magnetic field unlike diamagnetic materials which have negative susceptibility [7].

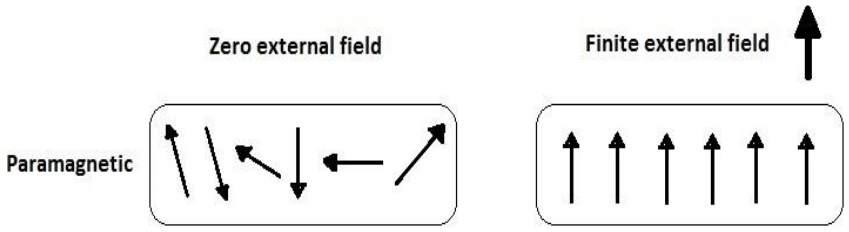

Figure 1.6 Para magnetic material Atomic dipole configuration [7]

1.10.3 Ferromagnetism

Iron, rare-earth and actinide elements are known ferro magnets, the atomic magnetic moment of these elements are aligned in a common direction under a specific temperature which is known as curie temperature [2]. Ferro magnets also show magnetization in the absence of an external field. Like paramagnetic materials ferromagnetic materials have also a positive susceptibility and attracted by the external fields. When a ferromagnetic material is placed in an external magnetic field under the curie temperature, the atomic magnetic moment of all atoms aligns themselves in the direction of applied external field and when the field is removed the atomic magnetic moment remains in that direction and the material shows magnetization in the absence of external field. When the temperature increases from the curie temperature for a ferromagnetic material then it shows paramagnetic properties. The ferromagnetic material has high saturation magnetization because of rapid increase in magnetization even in the presence of weak external magnetic field. Elements from the periodic table like Fe, Co, Ni, Sr and Br show ferromagnetic nature [2].

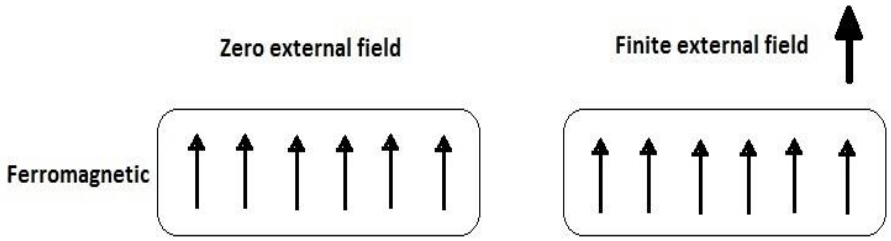

Figure 1.7 Ferromagnetic material Atomic dipole configuration [7]

1.10.4 Ferrimagnetism

In Ferrimagnetic materials the magnetic moments of all adjacent atoms are in opposite direction as it is in antiferromagnetic materials. The magnetic moments of adjacent atoms are opposite in direction but are not equal in magnitude unlike in case of antiferromagnetic materials in which the magnetic moments are opposite as well as equal in magnitude. Ferrimagnetic materials, under curie temperature hold spontaneous magnetization just like ferromagnets and they loss their spontaneous magnetization as the temperature increases from curie temperature and have no magnetic order [5].

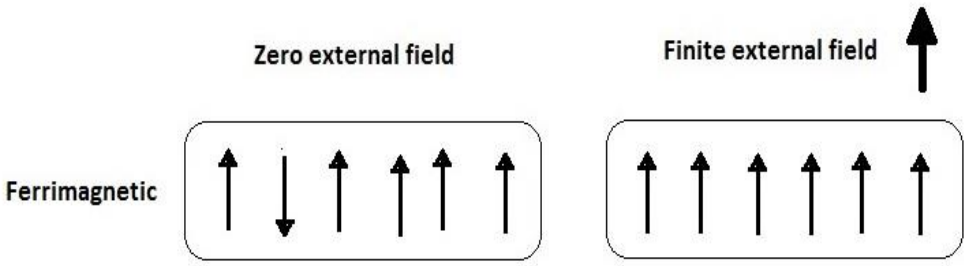

Figure 1.8 Ferrimagnetic material Atomic dipole configuration [7]

1.10.5 Anti-ferromagnetism

It results by the antiparallel arrangement which occurs between the spin of electrons of the neighboring atoms. A crystal consists of two lattices under anti-ferromagnetic behavior for which one is magnetized in one direction and the second is magnetized

in another direction. Anti-ferromagnetic behavior was first observed in MnO in 1938. When the external field is not applied then the magnetic moment of neighboring atoms cancels each other and the material show no net magnetization. And when the external field is applied some of the dipoles align in that direction of applied magnetic field and show small net magnetization. And this magnetization will increase with increasing temperature until a critical temperature is achieved which is called Neel temperature. This behavior exists at low temperature and diminishes above the Neel temperature. The examples of Anti-ferromagnetic materials are MnO, NiO, Cr, FeO and CoO etc. Such materials are called antiferromagnetic and such behavior is called anti-ferromagnetic behavior [2].

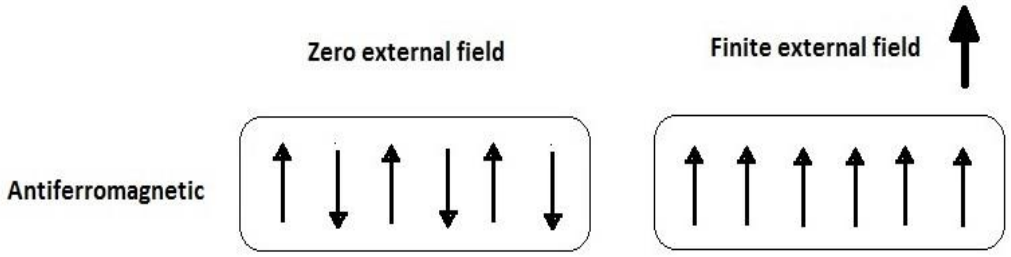

Figure 1.9 Antiferromagnetic material Atomic dipole configuration [7]

1.10.6 Super -para magnetism

It is a phenomenon in which the materials exhibit a paramagnetic behavior under the Curie temperature or Neel temperature. The temperature at which the ferro-magnetic or ferri-magnetic behavior is converted into paramagnetic behavior is called Curie temperature. In such materials, the coupling force causes the magnetic moment of neighboring atoms to align and results in a large internal magnetic field. The magnetic susceptibility of converted paramagnetic behavior is much larger than that of paramagnets.

1.11 Application of ferrites

Ferrite is important magnetic material due to their high resistive values. They have many applications at high frequencies. They are cheap and have high DC electrical resistivity, high coercivity, good magnetic properties, low eddy current losses,

mechanical stiffness. They have wide selection of materials and are also chemically stable over wide range of temperature. Because of such properties, ferrites has its applications in many areas such as recording tapes, magnetic devices, permanent magnets, switching devices, color imaging, flexible recording media and hard disc recording media, are also used to make transformer cores, permanent magnets and in other so many applications [3].Ferrites are widely used in the following applications:

- Microwave devices
- Drug delivery
- Data storage
- Electromagnetic absorbers
- Core material
- Ferro-fluids

1.12 Objectives

The present work is carried out with following objectives:

- Synthesis of single-phase spinel ferrite nanoparticles of $CoFe_2O_4$ using an inexpensive and simple chemical Co-precipitation
- To synthesize $CoFe_2O_4$ with Ag at varying concentrations
- To Study effects of Ag on $CoFe_2O_4$ ferrite nanoparticles dielectric and electrical properties.

Chapter 2

Literature Survey

Many researchers have approached different methods to synthesis the ferrite Nano particles loaded with some of other elements holding different characteristics and studied their combined properties for their respective applications. In the past few years a number of different processing methods were approached to synthesis these particles and cost-effective method. A brief summary of the literature survey is shown below:

Sinko et al in 2012 synthesized the Nano particles of cobalt ferrite via co precipitation route and studied the effects of parameters taken during experiment on the size of particle, size distribution with XRD, chemical composition and morphology of particles [25].

Easwari et al in 2014 did study on the cobalt ferrite Nano particles after synthesizing by co precipitation way Cubic spinel structure of cobalt ferrite in the powder was confirmed from XRD results also average particle size were calculated using Scherrer formula which was in the range of 8-10 nm. FTIR confirmed the functional groups and also analyzed. SEM provided the morphological analysis [26].

S.Sathiya et al in 2015 used co precipitation method to successfully synthesized the Nano particles of cobalt ferrite .they confirmed the presence of functional group presence on the tetra and octahedral sites with FTIR spectra confirming the spinel structure .other studies including size which was 24 nm and nearly spherical shape pf particles along with morphology confirmed from XRD and SEM respectively [27].

D.Sophia et al in year 2016 studied the Morphology and shape of cobalt ferrite Nano particles which was spherical in appearance and with uniform distribution by SEM images. they calculated the average size of the particle form XRD result which was 16 nm confirming successful synthesis of cobalt ferrite particles. They also applied FTIR to confirm the presence of functional groups. EDAX was implied to find presence of O, Fe, Na, C, Co [28].

Manju Kurian et al in 2015 prepared the single-phase cobalt ferrite Nano particles using co precipitation method and studied the influence of conditions like annealing

temp. acidic properties. after that particle size calculated from XRD data in the range of 21 nm and 30 nm at 450 ℃ and 750 ℃ respectively. FTIR was used to confirm the spinel structure while SEM images confirm the spherical shape and nanometer size of particle. Using VSM it was confirmed magnetic properties like saturation Magnetization, remanence, coercivity of cobalt ferrite depends on the parameter of method and temp [29].

Sonia Jovanovic et al in 2011 investigated the pH effect on properties as magnetic and structural of cobalt ferrite prepared using co precipitation method and got result as crystallinity enhance with pH along with Magnetization, remanence and Coercivity. Structural and size determined from XRD while SEM images provided morphological distribution in accordance with XRD in nanometers scale. [30]

Shayam M. Kodape et al in 2012 presented their study of cobalt ferrite Nano particles in which they include the particles in the size of 40 nm calculated from XRD data which was perfectly in agreement with SEM images outcomes. Also, agglomeration can be avoided using ethanol while washing. Size and distribution of particles can be controlled by varying temperature and reaction time during co precipitation

Kishwar khan in 2014 presented the magnetic study of cobalt ferrite synthesized via co precipitation also enhanced particle size along with distribution confirmed from XRD and SEM also backed those findings and cation distribution by FTIR. Absorption of electromagnetic waves is also studied and got reflection loss less than -18 dB hence provided this material good application in microwave antenna [31].

Gustavo B. Alcantara et al in 2013 studied the dielectric properties of cobalt ferrite Nano particle which were synthesized in enhanced particle size and distribution confirmed from SEM images and XRD data. These properties of permittivity and dissipation factor were studied by pressing the powder of cobalt ferrite Nano particles in pellets. Their application clearly be seen in chemical sensors [32].

N Sivakumar et al in 2007 studied the di electric behavior of Nano particles of cobalt ferrite and found that real portion of dielectric constant for 8 nm grain is higher than that of bulk .and this di electric constant decrease with increase in grain size and this is due to the migration of Fe^{3+} from octa to tetrahedral sites. Samples which were annealed activation energy for die electric relaxation is decreased. Die electric

properties can be controlled according to our requirement and specific application by controlling the grain size [33].

Sandhya Singh et al in 2017 studied the properties of cobalt ferrite like electric, dielectric, conductivity impedance etc. and enhancement in them with decrease in particle size calculated using Scherer method. also noticed the effect of factors like reaction time, stirring, temperature on the size and distribution of particles [34].

A.B Shinde in 2013 prepared the cobalt ferrite confirmed the single phase of these particles with XRD calculating the particle size using Scherrer formula from high intense peak of 311 ranging 27 nm. Electrical properties measured and noticed that Ac conductivity increase with frequency. The DC resistivity obeys the Arrhenius plot as it decreases with increasing temperature [35].

M.Krishna Surendra et al in 2011 co precipitation method was implied to synthesize the cobalt ferrite Nano particle of the size of average 20 nm confirmed from XRD because of Ostwald ripening there is increase in particle size with higher thermal energy. With increase in grain size the dielectric constant also increases. One semi-circle in the cole-cole plot agreed contribution to conduction is one. DC conductivity increases with grain size and it only due to grain size effect [11].

S.sumathi et al in 2017 synthesized the Nano particles of Cobalt ferrite, and copper co-substituted cobalt ferrite . Utilizing XRD, FTIR and SEM-EDX single pure phase was confirmed. copper ion decreases the lattice parameter and particle size of cobalt ferrite. From SEM images spherical shape of particle with agglomeration agreement with XRD can be seen. While at different concentration dielectric constant and dielectric loss increase [10].

Rakesh K. singh et al in 2012 synthesized the copper substituted cobalt ferrite nanoparticles. cubic spinel structure and single phase confirmed from XRD. While it is perfect match with both $CuFe_2O_4$ and $CoFe_2O_4$ JCPDS cards and lattice parameter also match. The bonds vibration like Co-O, Cu-O and Fe-O were shown by FTIR spectra. Dielectric properties also enhanced with addition of copper [36].

Balavijayalakshmi j et al in 2012 utilized co precipitation method to prepare copper loaded cobalt ferrite $Co_{(1-x)}Cu_xFe_2O_4$. FTIR confirmed the vibration due to stretches of Octa and tetrahedral complexes and formation of cubic spinel structure was

attributed from XRD along with the calculation of Crystallite size ranging 37-52 nm. As it decreases with increase concentration of copper. Magnetic properties like remanence, magnetization and coercivity also decrease with increase copper concentration [37].

Sheena Xavier et al in 2014 synthesized the silver loaded cobalt ferrite $Co_{1-x}Ag_xFe_2O_4$. Formation of spinel structure along with the varying size from 15-20 nm were exhibited from XRD results' spectra also seen in agreement with the Spinel structure. The magnetic properties decrease with increase in concentration initially the increase and decrease is due to silver particles on octahedral sites which are nonmagnetic in nature [38].

Raul Valenzuela in 2011 presented the wide range of applications of ferrites which includes recording and microwave devices due to magnetic nature from past 50 years but now with advances in Nano technology they are getting more and more interesting with medical application and other composite of ferrites may utilized for EMI shielding etc [3].

Chapter 3

Synthesis and Characterization techniques

3.1 Approaches

Ultrafine dimensions of the order of 10-9 have been found in nanostructure materials. At this lower scale, several approaches may be implemented in the fabrication of the nanostructure material [13]. Following two approaches are utilized for synthesizing of Nano material and the manufacturing of Nano structure in nanotechnology;

- Top down approach
- Bottom-up approach

3.1.1 Top down approach

The manufacturing of nanoparticles with the implementation of top down approach involves the construction of material by continues removal of material until required material is obtained by using the methods such as carving cutting, and molding. By applying these approaches, we succeeded to manufacture a range of machinery and electronics devices. Following is a list of methods which are applied for the production of Nano-scale materials

- Ball milling
- Nano-lithography
- Laser ablation

3.1.2 Bottom up approach

The fabrication of Nano material and nanostructures with the bottom up approach starts with single molecule, which are combined together in the form of: atom by atom, molecule by molecule or cluster by cluster. Different methods used in the bottom up approach are [4]

- Co precipitation method
- Sol gel method
- Double solvent sol gel method

- Hydrothermal method.

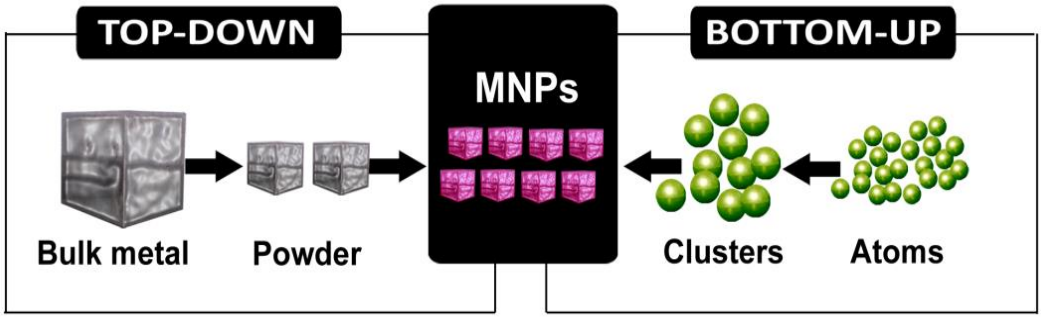

Figure 3.1 Top Down and Bottom Up approaches [57]

3.2 Synthesis methods

As the ferrites are very useful in different applications as discussed in their Nano size. The researchers discovered a lot of methods which are used to prepare ferrites nanoparticles each one has some advantages and disadvantages too. The various methods of synthesis possess different magnetic, structural and electrical properties. Different methods which are used to prepare ferrite nanoparticles are listed below.

- Hydro-Thermal
- Sol-Gel
- Micro-emulsion
- Solvo-Thermal
- Sono-Chemical
- Co-precipitation

3.2.1 Hydro -Thermal/Solvo-Thermal method

The hydro-thermal/solvo-thermal method is used because of its simplicity, low cost, and remarkable morphology of the prepared Nano ferrites. The hydrothermal/solvo-thermal method is used to synthesize the crystalline structures (single crystals and films etc.) under high vapor-pressure from the aqueous solution. By controlling the growth of particles and the solution re-crystallization results in the production of various morphological crystals i.e. Nano-spheres, nanorods, nanocrystals, Nano-cubes, hollow spheres, Nano-rod bunches and urchin-like crystals.

3.2.2 Sol- Gel method

The sol-gel technique [35] is consist of two steps of alkoxide based precursor. These two steps are hydrolysis and condensation. In sol-gel a liquid solution is prepared from the initial material and then a solid gel is obtained from that liquid by using a chelating agent, then this solid gel is converted into required product by the process of annealing. In this method the size of particles depends upon the composition of sol, its pH and the temperature on which the reaction is carried out. This technique consists of a number of different steps. The temperature provide in sol gel for the purpose of annealing is not that much high but it required a lot of time for its completion. Moreover, the chelating agent used for gel formation, is also become a reason for the presence of impurities in the product. The materials which are made through this technique have wide applications in optics, electronics and energy etc.

3.2.3 Micro-Emulsion method

In micro-emulsion method, a surfactant is dissolved in an organic solvent which form aggregates of spheroidal shape which are named as "reverse micelles [7]". These micelles are in fact 'water in oil' micro-emulsions where the tiny drops of water are surrounded by the molecules of surfactant and thus forming a water pool. The water pools of such micelles act as micro reactors in which the particle size is controlled by the size of these pools. Precipitation in micro-emulsions is very useful for the preparation of ultra-fine ferrite nanoparticles for the controlled size and morphology. The microemulsion method is very costly as compared to other methods, it requires large quantity of liquids and also the annealing temperature is very high.

3.2.4 Sono-Chemical method

In sono-chemical method, the starting materials are chemically reacted under high frequency ultrasonic waves which have been employed for several purposes; fabrication of nanostructured materials in various organic and inorganic reactions. This method has advantages of the reduction of the growth of crystal, the morphological control and uniformity of mixing.

3.2.5 Co-Precipitation method

This method uses a very short time to synthesis the nanoparticles while the disadvantage of this method is the emission of fumes. Its reaction revolves around the nucleation, growth, coarsening and agglomeration process of the nanoparticles. When

the precipitation starts; the nucleation of small crystallites forms which tends to grow together to form larger crystallites [11]. To make the nanoparticles, the nucleation should be fast enough to slow down the growth process. The reaction process for the synthesis of oxides is divided into two categories; one that make oxides directly and the other that make a precursor which require further processing i.e. drying and calcinations. A base solution of ammonium hydroxide solution or sodium hydroxide is additionally used to form the metal hydroxides. The resulting chlorides are washed away and the hydroxide is washed and filtered followed by calcinations to obtain the final product. Co-precipitation is a very useful technique to obtain the fine nanoparticles. The product obtained from this method is pure and homogeneous in chemistry. After adding sodium hydroxide, the formation of oxide nanoparticles depends on the control of pH value. The particle sizes of the nanomaterials depend on the pH of the starting precursors. Molarity of the chemicals also controls the particle size of the nanomaterial. The transport and chemical rates are affected by the concentration of the chemicals. The crystallinity of the particles is affected by the reaction rates and the impurities. The particle size is affected by nucleation, growth rate and super saturation. The particle size is small at high super saturation. Sodium hydroxide is mostly used as precipitating agent. A reasonable value of pH and temperature is required for the precipitation purpose.

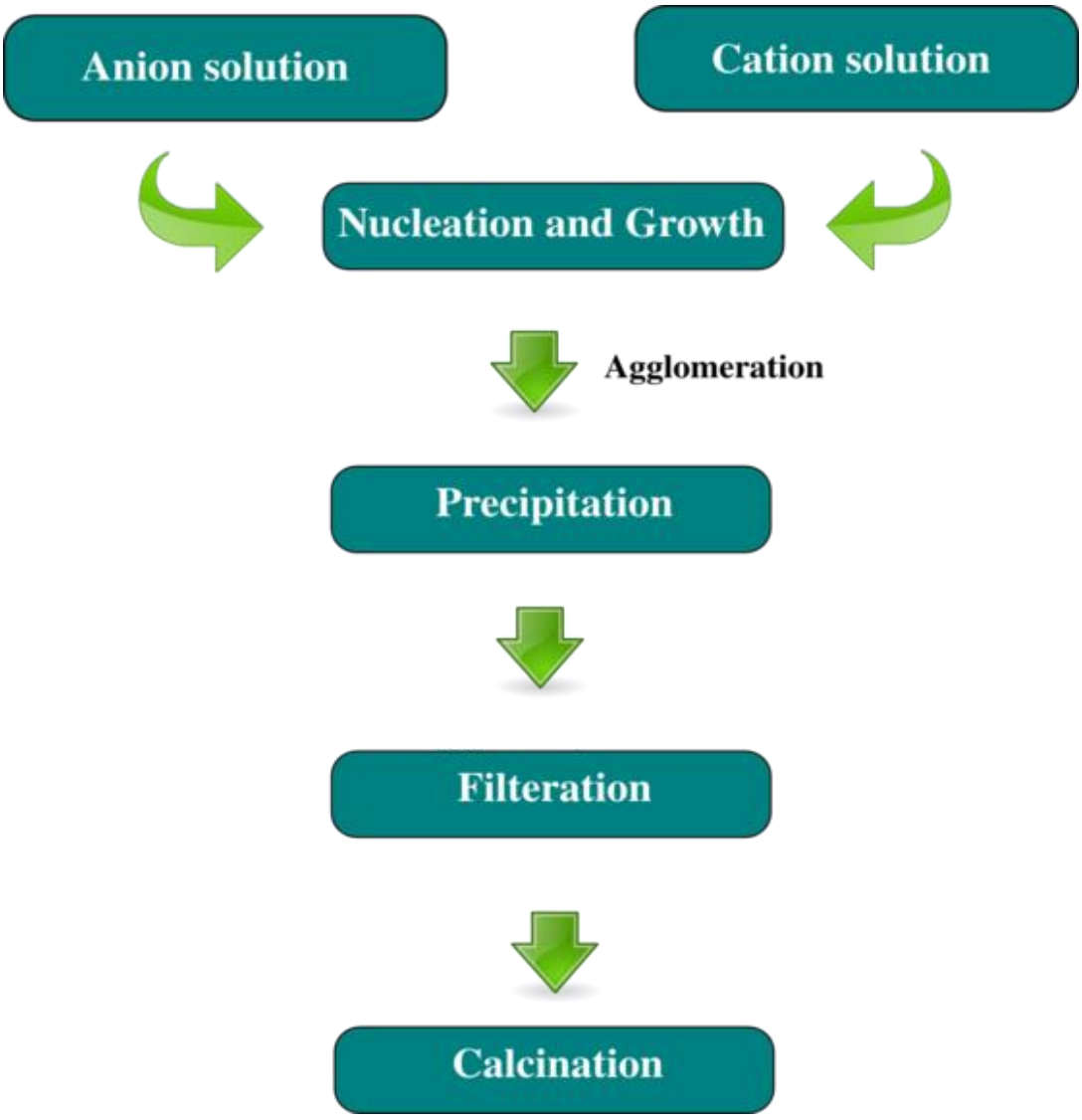

Figure 3.2 Chemical co precipitation steps [40]

3.3 Major steps in co-precipitation

Two major steps involved in co-precipitation are [39]

- Co-precipitation step
- Ferritization step

3.3.1 Co-precipitation step

At first solid hydroxides of metals in the form of colloidal particles are obtained by the co-precipitation of metal cations in alkaline medium [4].

3.3.2 Ferritization step

Then this product is subjected to heating in the precipitation alkaline solution to provide the transformation of metal hydroxides solution to the Co ferrites. In co-precipitation process some parameters have great influence on the precipitate formation and the size and shape of the particles formed. The ionic impurities of Na and NO_3 are removed by washing the product with deionized water until the pH value reaches to neutral. [1]

3.4 Parameters effect the co- precipitation method

Some parameters and their influence on the co-precipitation process can be described as [40]

- Rate of mixing of the reactants
- Role of anion
- Temperature effect
- Effect of pH
- Heating after co-precipitation

3.4.1 Rate of mixing of the reactants

The rate of mixing greatly influenced the size of the particles. Nucleation and growth are the two important processes in the co-precipitation process. Small size particles are formed when the growth rate is slow and the nucleation rate is higher than the growth rate. In the same way the large particles are formed when nucleation rate is low as compared to the growth rate. In first case the rate of mixing of the precursors is very high and in the second case rate of mixing is low [30]. Slow mixing gives the particles of homogeneous chemistry. This shows that if the mixing rate is high then small particle size is formed and if the mixing rate is low then the large particle size is formed.

3.4.2 Role of Anions

The properties of the nanoparticles depend on the types of anions which are used in the co-precipitation method. Anions can be metal salts or metal ion solutions. The metal salts are used for the good result. The examples of metal salts are nitrates, sulphates and chlorides etc. In the presented work, the metal salts of nitrates are used for the synthesis of the cobalt ferrite.

3.4.3 Effect of temperature

Different metals have the different values of activation energy for the ferrite's formation. The activation energy is obtained from the heat given to the reactants. For the formation of cobalt ferrites use mostly use the reaction temperature in the range 70-100 centigrade.

3.4.4 Effect of pH

pH plays an important role in the synthesis of controlled size and shape particles. At low values of pH, the growth of the particles is no significant. On increasing the value of the pH, the growth rate of the particle yield is high enough. Increase in the pH value decreases the time required for the synthesis of the product. In our case of Cobalt ferrites, the pH range is 11-12.

3.4.5 Heating after co precipitation

When the co-precipitation process is completed for the formation of the required phase annealing is required. The particle size depends on the duration of heating at the soaking period of the annealing process. In the presented work, the duration of heating was 45 minutes.

3.5 Chemical Used

- Cobalt Nitrate
- Iron Nitrate
- Sodium Hydroxide
- Silver nitrate
- Copper Nitrate
- De ionized water

3.6 Apparatus and Glassware used

- Beakers
- Hot plates and Magnetic stirrer
- Oven
- Aluminum foil
- China dish
- Furnace

3.7 Synthesis Procedure

For the preparation of nominal composition $CoFe_2O_4$, the chemical reagents used for Coprecipitation were iron nitrate $Fe(NO_3)_2.9H_2O$ and Cobalt nitrate $Co(NO_3)_2.6H_2O$ with NaOH to control the PH to about 11-12 for the co precipitation of metal

hydroxide to occur, which is then subsequently neutralized by washing the sample with de-ionized water. The respective composition was made using the simple stoichiometric formula:

$$\boldsymbol{Mass = \frac{Molarity \times Molecular\ Mass \times Volume}{1000}}$$

In this process first of all the stoichiometric amount of 0.2M (300ml) Fe $(NO_3)_3.9H_2O$, 0.1M (300ml) Co $(NO_3)_2.6H_2O$ and 3M (300ml) NaOH were dissolved in double distilled de ionized water in separate beakers with the help of magnetic stirring. After obtaining crystal solutions, the crystal solution of Co $(NO_3)_2.6H_2O$ is mixed with Fe $(NO_3)_3$ $.9H_2O$ and again stirred for another 15 minutes at room temperature. After that the temperature was increased to 90^o C of the mixed solution and stirred vigorously and kept at that temperature. After that crystal solution of NaOH at the same temperature was also mixed dropwise to Co $(NO_3)_2.6H_2O$ and Fe $(NO_3)_3$ $.9H_2O$ solution and a mixed solution was obtained having pH value equal to 12. Then the solution was kept at 90^o C for another an hour and stirred vigorously and the pH was kept at 12-13 pH value. After an hour the heating was turned off but the stirring was kept ON till cool down of product to room temperature.

In the result of above procedure, a black colored solution was obtained which was then washed several times with double distilled de ionized water until the pH value 7 was obtained. After washing the sample was kept in oven for overnight drying on 100^oC. Then the obtained product was crushed grinded by mortar and pestle and converted into a fine powder. Then the powder was kept in a muffle furnace for 8 hours at 800^oC for annealing. After annealing the final product was again crushed into fine powder [41]. Similar procedure is repeated for the loading Ag the only thing we have to change and kept is combined molarity of nitrate salts Ag and Cobalt must be 0.1 according to formula the rest of the procedure is same for all The resultant powder was grinded using Mortar and Pestle to eliminate agglomeration and the powder was characterized using X-rays powder Diffraction, Fourier Transform Infrared

Spectroscopy , Two Probe Method ,Scanning Electron Microscopy and RLC impedance analyzer . Following is the schematic for the whole process.

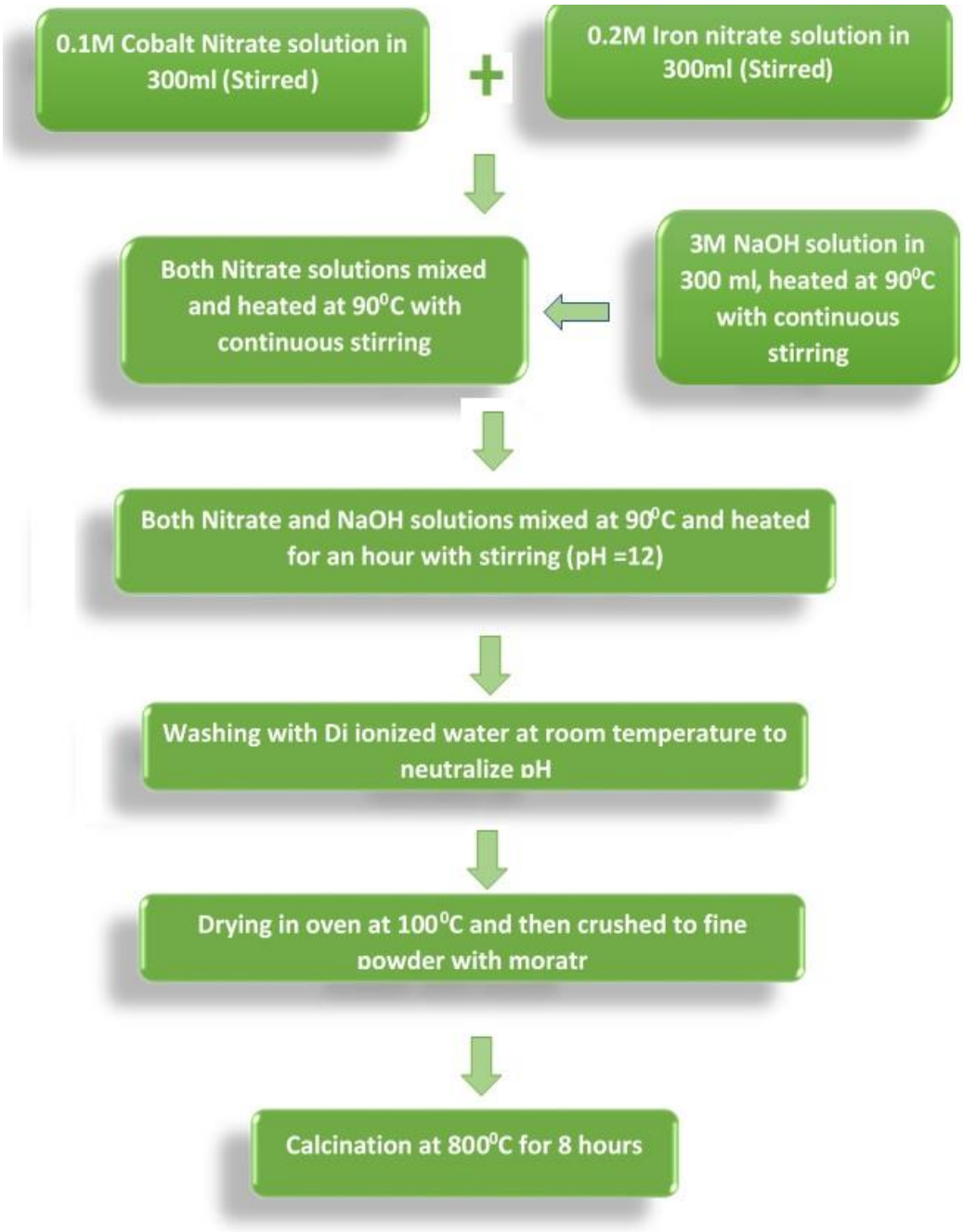

Figure 3.3 Schematic of Synthesis

3.8 Characterization Techniques

There are many characterization techniques which are used to study the properties of any material. But in this work the following characterization techniques are used to study the properties of cobalt ferrite and Ag loaded Cobalt ferrite.

X-Ray Diffraction

- Phase formation
- Crystallite Size
- X-ray Density
- Porosity

Scanning Electron Microscope

- Surface morphology
- Structural observation

Fourier Transformed Infrared Spectroscopy

Impedance Analyzer

Dielectric properties

AC Conductivity

AC Impedance Spectroscopy

3.8.1 X Ray Diffraction (XRD)

X-Rays diffraction technique was discovered by W.C. Rontgen in 1985. It is very useful technique to study the structural properties of crystal. In crystal there is the huge difference between the slit size and the huge variation in the light wave, the light rays are not suitable for structural properties. On the other hand, x-rays wavelength is approx.: equal to the slit size of crystal, that's why this method was discovered. It provides us information about structures, phases, crystals orientation and parameters like average crystallite size, structural strain, degree of crystallinity and crystal defects. There are different methods to determine crystal structure like Laue method, rotating crystal and powder diffraction method. Size of the crystal can be determined by the powder diffraction method by two different techniques [42]:

- Debye Scherrer Method

- Diffractometer Method

The target material can be of various type of target materials like Copper and Molybdenum etc. in this research we used Cu - kα = 15.4 nm as XRD source.

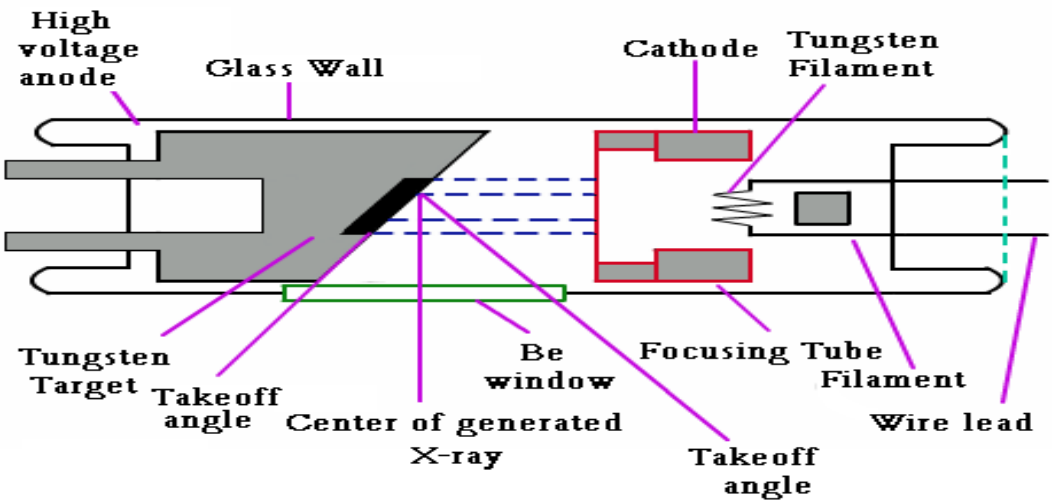

Figure 3.4 X ray production [42]

3.8.1.1 Working principle of XRD

The X-Ray beam hit the sample and crystal planes which acts as mirror reflect that beam and the angle of their reflection equals to the angle of incidence which in other terms known as constructive interference. This interference in each set of atoms cause the interference of x-rays within the crystal [42]. The phenomenon of interference can be defined by Braggs Law which is given by:

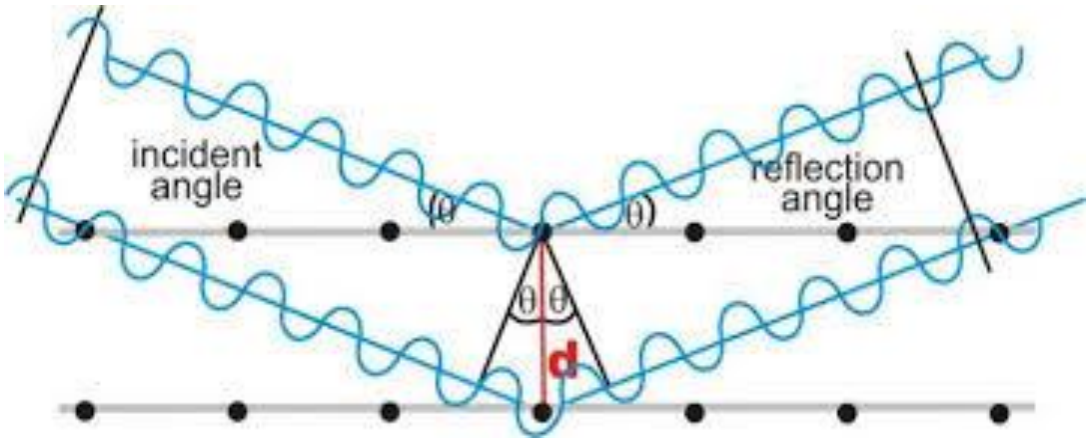

Figure 3.5 Bragg's Law [42]

$$n\lambda = 2dSin\theta$$

n=Interference order

θ=Angle of incidence

d=Interlayer distance

λ=Wavelength of incident X-rays

Bragg's law says that the radiations are reflected from the path difference of 2dsinθ which are subjected to equally spaced planes at a distance of 'd' and 'θ' is measured from plane. The constructive interference can be formed. For the above-mentioned equation reflection can only occur when λ<2d which is the reason why visible light cannot be used. There are three techniques which are commonly used for XRD characterization.

- Laue Method
- Rotating Crystal Method
- Powder diffraction method

As the prepared sample is composed of Nano powder we use powder diffraction method. This method is best suitable when single crystals are not available of acceptable sizes. For this method, the prepared sample powder is grinded finely to a small size and then place in a circular plate of aluminum of glass. The X-Rays are hit on prepared powder which is randomly oriented with respect to the x-rays. In powder method, the forming of a diffracted cone. For a particular reflection, some of the nanoparticles are aligned in such a way that their (hkl) planes form the perfect Braggs angle

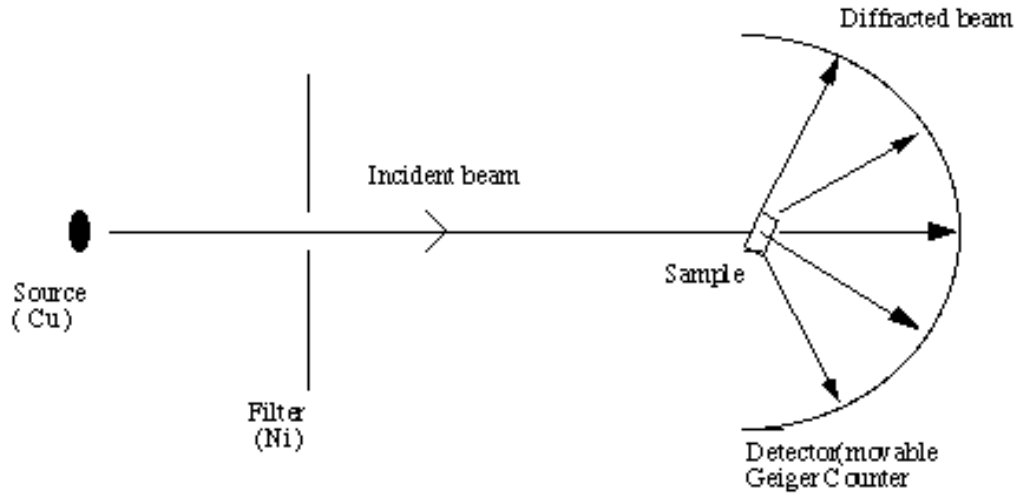

Figure 3.6 X ray diffractometer [58]

3.8.1.2 Lattice constant

It is a parameter which shows the length of one of the edges of the unit cell of crystal lattice. It is also termed as lattice parameters. It refers that the distance between lattice points is constant. It is calculated by the equation given below:

$$\boldsymbol{a = \frac{n\lambda}{2Sin\theta}\sqrt{(h^2 + k^2 + l^2)}}$$

Where "a" is lattice constant, "λ" is the wavelength of X-rays, (hkl) are the miller indices and "θ" is the diffraction angle.

3.8.1.3 Crystallite Size

The crystallite size has great impact on the structural properties of the material. The diffraction patterns which are obtained through experimentation are verified and compared to JCPDS cards for phase confirmation and identification. The peak broadening effect in XRD relates to small and large crystallite size [42]. The average crystallite size was calculated by Debye-Scherrer formula which shows that peak width is inversely proportional to crystallite size as shown below:

$$\boldsymbol{t = \frac{0.9\lambda}{\beta Cos\theta}}$$

Where "λ" is the wavelength of the X-rays, "θ" is the diffraction angle and "β" is FWHM value of respective peaks.

3.8.2 Scanning Electron Microscope (SEM)

The morphological studies are performed by the scanning electron microscopy. A high-energy electron beam is thrown upon the surface the samples. The interaction of electron with the sample gives rise to different types of signals that give the morphological information of the sample. Magnification range 15x to 200,000x. This has the resolution in the range of angstrom Å. It has excellent depth of focus. It has relatively easy sample preparation. After the interaction of electron beams with surface of sample, it generates various types of signals which are; auger electron, secondary electron, back scattered electron, transmitted electron, x-rays and cathodoluminescence.

3.8.2.1 Working principle

It contains the following parts

3.8.2.2 Electron Guns

The electron gun is placed either at bottom or at top of SEM and these guns shoot a beam of electrons at the object to be studied [49].

3.8.2.3 Condenser lenses

SEM uses these lenses to create comprehensive and thorough images. The lenses are not made up of glass but of electromagnetic material [43]. These lenses are used to control and focus beam of electron to ensure their precise targeting.

3.8.2.4 Objective aperture

The objective aperture arm lies above the objective lens and it contain four holes. By the motion of the arm, different sized holes can be adjusted to put into the beam path.

3.8.2.5 Scan Coils

The scanning coils are basically the two solenoids that are used to create two magnetic fields perpendicular to each other. By varying the current, a magnetic field is generated that controls the movement of electrons.

3.8.2.6 Chamber

The sample chamber is a place where the specimen is kept for examining. By moving the chamber, different images are taken

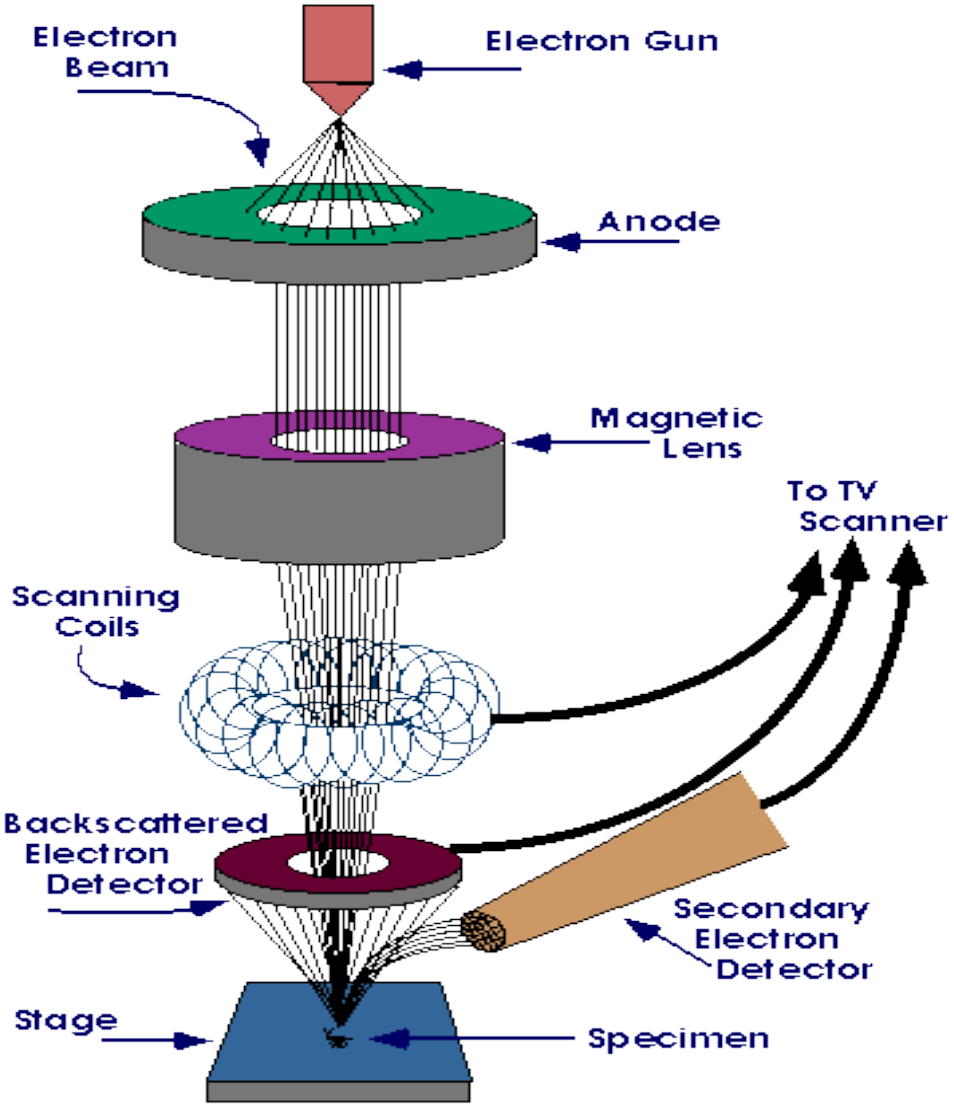

Figure 3.7 Construction of SEM [59]

3.8.2.7 Detector

SEM contains various types of detectors. These detectors detect the various types of signals by the interaction of electron beam with the sample. Different types of detectors are backscattered electron detectors and X-ray detectors [43].

There are different types of electron images.

- Secondary electrons emission
- Backscattered electron emission
- X-rays emission
- Electrons back scattered diffraction

In the scanning electron microscope, the high energy beam of electrons is focused to the surface of sample by using some pairs of magnetic lenses. In the last lens, beam is deflected in the x and y direction to scan the rectangular area of the sample surface in order to control the brightness of the resulting image. The vacuum is produced in the chamber to prevent from defocusing of electron beam and contamination of dust particles. When the electrons interact with the surface of sample, it emits various types of electrons from the surface. Different types of detectors are used to collect these various types of electrons. For every type of electron there is a different detector. The most common detector for SEM is used for secondary electrons.

3.8.3 Fourier transformation infrared spectroscopy (FTIR)

The presence and identification of chemical bond in a sample is found by using "Infrared Spectroscopy". In IR spectroscopy, the sample is irradiated with a full range of infrared frequencies. The infrared frequencies are absorbed by those molecules which vibrate with the similar frequencies. By absorption of infrared frequencies, the molecules get excited and in a short time they again deexcite to find stability which occurs in less than 10^{-6} seconds [44]. The energy released by molecules may be in the form of kinetic energy or in the form of photons. This absorption of frequencies of infrared light is measured by the spectrometer as a function of wavelength of light behind a sample. A transmittance or absorbance spectrum is plotted from the lack of intensities found at the molecule's vibrational frequencies and the chemical bonds present in the sample are determined through this way. Fourier transformation infrared spectroscopy (FTIR) is a similar technique to IR spectroscopy. In FTIR an interferometer is used which split the IR radiation two beams having different optical distances which creates "alternating interferences fringes". One of the most common interferometers is "Michelson interferometer". A Michelson interferometer consists of the following main arms [44].

•Infrared radiation source arm
• Stationary mirror arm
• Moving mirror arm
• Open arm

At the intersection of these four arms a beam splitter is placed which split the IR beam into two beams. Half of the IR beam pass through the beam splitter and falls on the fixed mirror where the remaining half strikes on the moving mirror. These two beams reflect back from the fixed and moving mirror respectively and combine again and then strike on the sample and then detected by the detectors [44].

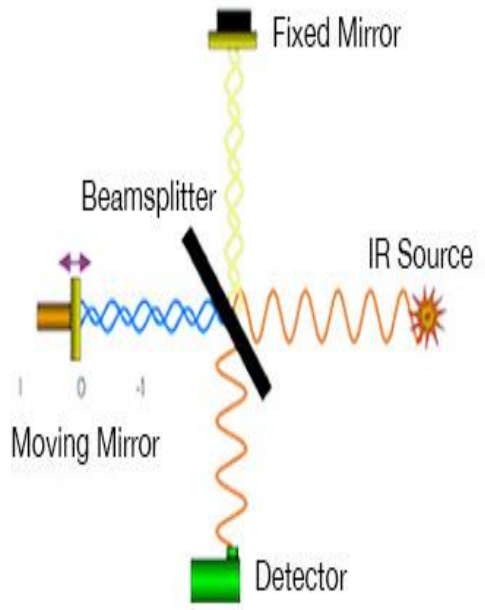

Figure 3.8 Michelson' Interferometer [46]

The two beams reflected back from their respective mirror form a constructive interference pattern or destructive interference pattern depending on the length of the path provided by the moving mirror [44]. FTIR spectroscopy become very useful technique as compare to convectional spectrometer, because it is a very economical, very sensitive and provide complete information about the sample in whole range of frequency in a very short time [57].

Figure 3.9 FTIR [46]

3.8.3.1 Uses

FTIR is a widely used technique. Following are some characteristic features of FTIR spectroscopy.

A small instrument and can carry easily from one place to other

• Give accurate measurements with the help of computer filters and results manipulation

• Can store a wide range of reference spectrums with which one can easily compare spectrum obtained from his sample.

• Can be used both for organic and inorganic materials

• Useful in verification and identification of sample

• Useful in the study of semiconducting materials

• Useful in measuring the degree of polymerization in polymers.

• Helpful in finding variation in quality of specific bonds

3.8.4 Dielectric properties

The dielectric parameters were measured using LCR Meter Bridge. Capacitance and d-factor was measured of the pellets and then dielectric constant was calculated by the equation [2].

$$\boldsymbol{\varepsilon' = \frac{C \times D}{A \times \varepsilon_0}}$$

Where "C" is capacitance, "D is dissipation factor, "A" is surface area of the pellets and "ε_0"is permittivity of free space.

3.8.4.1 Dielectric constant

is a property of the material that expresses the force between two-point charges. It is the factor by which the electric field is decreased between the charges relative to vacuum. The dielectric parameters can be explained according to Maxwell-Wagner model [45]and Koop's theory [46]

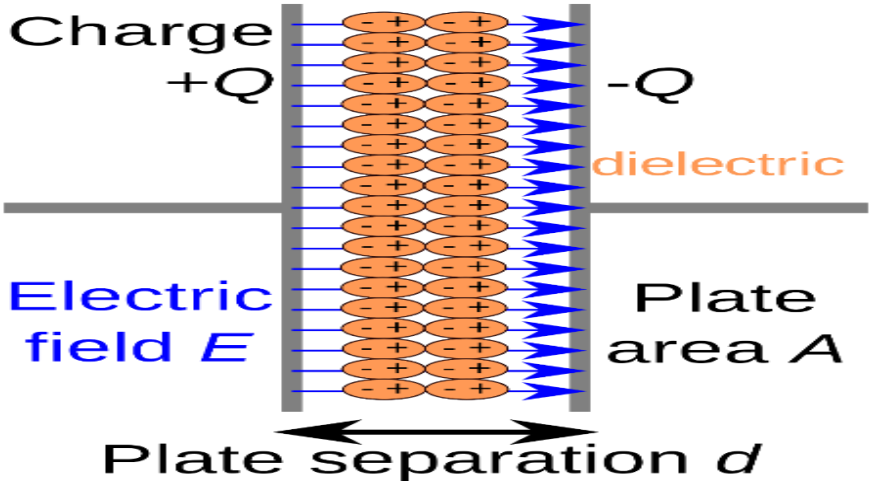

Figure 3.10 Dielectric Dipole [46]

3.8.4.2 Dielectric loss

(imaginary part of dielectric) corresponds to energy dissipation losses [46]. It was calculated by the equation

$$\varepsilon'' = \varepsilon' \times D \quad \text{or} \quad \varepsilon'' = \varepsilon' tan\delta$$

3.8.4.3 dielectric loss tangent

shows energy dissipation [47]. It is the ratio of dielectric constant and dielectric loss as shown by the equation

$$tan\delta = \frac{\varepsilon''}{\varepsilon'}$$

3.8.4.4 AC-Conductivity

resulting because of the hopping mechanism is calculated using the equation

$$\sigma_{AC} = \omega \varepsilon_o \varepsilon' D$$

3.8.4.5 AC impedance

parameters of the samples were measured at room temperature. Resistance (R) and reactance (X) were measured over a range of 100 Hz to 5 MHz frequency. The impedance is a complex quantity where resistance (R) and reactance (X) shows the real and imaginary parts of impedance in the circuit by the relation:

$$Z = \sqrt{R^2 + X^2}$$

The impedance shows the resistive behavior of the material. The SI unit of impedance is 'Ω'. The Cole-Cole plot of real and Imaginary parts of impedance shows contribution of resistance in the material.

Figure 3.11 LCR Meter

Chapter 4

Results and Discussion

4.1 X Ray Diffraction (XRD)

The XRD technique is very useful to estimate the structure and phase of the crystalline material and it also give information of cell dimensions. XRD is the key technique when we synthesize any material because it provides confirmation of the phase and structure.

The structure of Cobalt ferrite $CoFe_2O_4$ nanoparticles loaded with Silver Ag at different concentrations according to formula $Ag_xCo_{1-x}Fe_2O_4$ were study with the help of X-ray diffraction technique. This structure analysis was done by Cu K_α radiations of 1.5418Å and scanning angle 2θ where θ ranging from 20 – 80 degree.

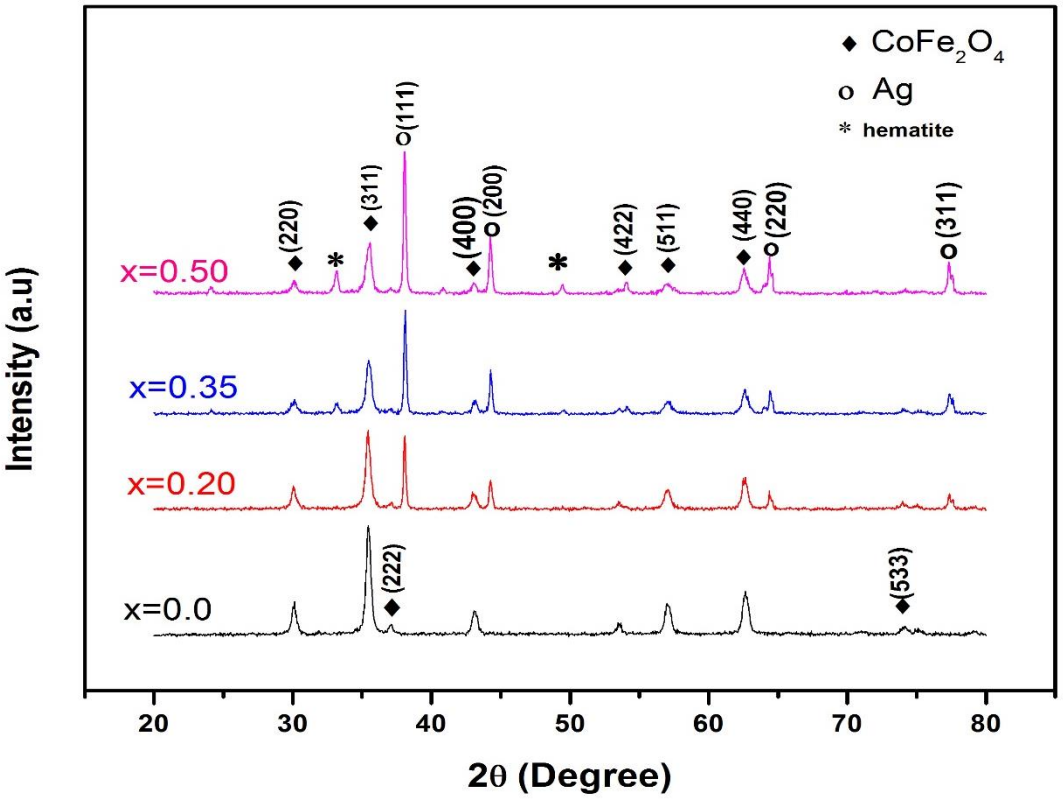

Figure 4.1 XRD graph of $Ag_xCo_{1-x}Fe_2O_4$ with increasing concentration (x) of silver

The XRD spectrum of $Ag_xCo_{1-x}Fe_2O_4$ nanoparticles is illustrated in figure 4.1 .The XRD data is in accordance with standard reference values recognized by the Joint

Committee on Powder Diffraction Standards as card no. 00-022-1086 for cobalt ferrite and card no. 03-065-2871 for metallic silver .The peaks of reflection confirms the achievement of cubic spinel structure while the additional peaks of metallic silver confirmed the presence of silver, reason for the most of silver remain as metallic is related to the ionic radii of both Co^{2+} and .it can be elaborated by comparing the ionic radius of Ag^{2+}(1.08Å) and Co^{2+}(0.70Å) Co ferrite crystal structure [38].silver ions as have greater ionic radii so silver ions cannot penetrate the spinel lattice of cobalt ferrite and form secondary phase [38]. At higher concentration of silver there is also peaks for hematite Fe_2O_3 in the Xrd pattern. The most intense peak was used for the determination of crystallite size of the XRD pattern which is (311) in our case. The average crystallite size for the sample was calculated by using the Scherer's formula. The crystallite size obtained for $Ag_xCo_{1-x}Fe_2O_4$ at x=0.0 means pure Cobalt ferrite $CoFe_2O_4$ is 31 nm while crystallite size ranges from 31 to 44 nm. With increasing concentration of silver Ag as x=0.0 , 0.20, 0.35, 0.50 results in decline of intensity of peaks which is clear from (311) peak and this decrease in intensity is due to the defects formed by the ion of Ag present in the lattice of ferrite [48].

The Full Width Half Maxima (FWHM), d spacing, cell volume. lattice constant is also obtained from the XRD spectra and calculated using relation mentioned in previous chapter. the cell parameters like d-spacing, lattice constant, cell volume decrease linearly with increase of Ag concentration following vegard's law [49]and also peak position also shifts to higher values also mentioned in table 4.1 and can be seen from spectra above 4.1, this linear decline in cell parameter may referred to change of Co^{2+} small ionic radii with larger ionic radii Ag^{2+} in Cobalt ferrite crystal system [48] Also, compression of lattice because of secondary phase on grain boundaries, and increase silver content also results in the accumulation of silver on the boundaries due to which expansion of spinel lattice is blocked [38]. Study on cation distribution in case of silver cobalt ferrite is required.

Table 4.1 XRD data for $Ag_xCo_{1-x}Fe_2O_4$ and its variation with concentration of silver

Sample (x)	**0.0**	**0.20**	**0.35**	**0.50**
Position [2θ] (311)	**35.44**	**35.46**	**35.52**	**35.63**
FWHM [2θ]	**0.2629**	**0.2424**	**0.2155**	**0.1867**
d-Spacing [Å]	**2.532**	**2.530**	**2.526**	**2.519**
Cell Volume ($X10^6 pm^3$)	**592**	**591**	**588**	**583**
Lattice Parameter [Å]	**8.400**	**8.393**	**8.380**	**8.356**
Crystallite Size (nm)	**31**	**34**	**38**	**44**

4.2 Fourier Transform Infrared Spectroscopy (FTIR)

Fourier transform infrared spectroscopy (FTIR) was done by illuminating the samples with infrared waves of wavelength (350-4000 cm^{-1}). The FTIR was carried out with the help of (Perkin Elmer-spectrum 100) FTIR spectroscope using KBr pellets [44]. It is an important mean to know the structure of spinel phase in the cobalt ferrite Nano particles. It provides us with information about the vibration modes and position of the bi and tri valent ions of metals. In the case of ferrite FTIR provide us data and absorption spectrum of IR is obtained due to vibrational modes involving oxygen ions along with cations occupying tetra and octahedral sites within the unit Cell.

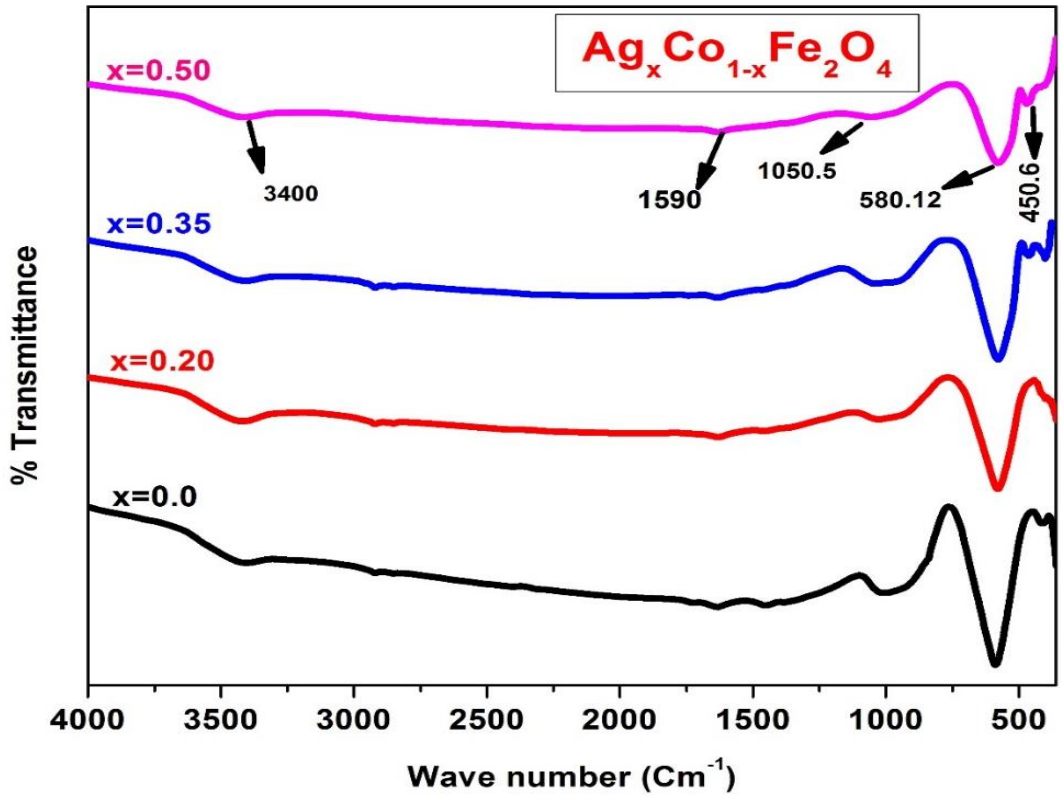

Figure 4.2 FTIR spectra for $Ag_xCo_{1-x}Fe_2O_4$ with increasing Concentration(x) of silver

The FTIR spectra for $Ag_xCo_{1-x}Fe_2O_4$ (x=0.0, 0.20, 0.35, 0.50) is also obtained in the range of 350-4000 cm^{-1}. For the spinel ferrites the characteristic absorption region is in the range of 380-600 cm^{-1}, Two distinguish bands can be seen in spectra of spinel ferrite which are of Metal- oxygen. Figure 4.2 shows FTIR graph for $Ag_xCo_{1-x}Fe_2O_4$. The band with higher frequency is located in the range of 550-600 cm^{-1} it refers to the tetrahedral sites having metal ions with oxygen stretching vibrations which represents ferrite phase while the other prominent frequency band is ranging lower frequency between 380-450 Cm^{-1} and this corresponds to the stretching vibrations of octahedral sites occupied by the metal ions ,all the samples under consideration exhibit these bands .It is also noted that with increase in the silver concentration the prominent bands move towards lower values. This can be explained by the fact that bond length change has a inverse relation with band frequency shift also formation of secondary phase in the case of silver [38]. Spinel phase structure is confirmed with two tetrahedral (A) and octahedral (B) lattices site [7], as we know cobalt ferrite have inverse spinel structure so in it Co^{2+} ions present on octahedral site so vibrations correspond to this site are due to Co^{2+}-oxygen while with addition of silver, it also

takes part in it by substituting Cobalt [10]. Tetrahedral stretching vibrations are due to Fe^{3+}-oxygen as it is present on the tetrahedral site. There are also small peaks near the 865 cm^{-1} confirming the presence of metal – oxygen vibrations, all the peaks in the range of 1100-1600 cm^{-1} corresponds to Co-O, and Fe-O vibrations .peak around 1050 cm^{-1} corresponds to the O-H bending vibrations while peak around 1600 cm^{-1} is because of OH^{-1} or molecular H_2O along with the peaks the peak at 3400 cm^{-1} is also attributed to O-H bond which confirms the presence of moisture in the sample while characterizing.

4.3 Scanning Electron Microscopy (SEM)

The morphological study of cobalt ferrite $CoFe_2O_4$, and Silver substituted $Ag_xCo_{1-x}Fe_2O_4$ (x=0.0,0.20,0.35,0.50) nanoparticles prepared by coprecipitation method was carried out by low vacuum scanning electron microscope (JSM-6490A), operated at 20 KV with magnification range 100X ~ 70000X. The samples were dispersed in ultrapure water with the help of ultra-sonication and when uniform dispersions were obtained then drops of dispersions were dropped on glass slide and then dried. The samples were gold coated of 25Å with the help of Sputter Coater (JFC1500) to made them conductive. The images taken by SEM in Figure 4.3 and 4.4 exhibits the morphology of ferrite nanoparticles which concurred the XRD results, providing spherical appearance of

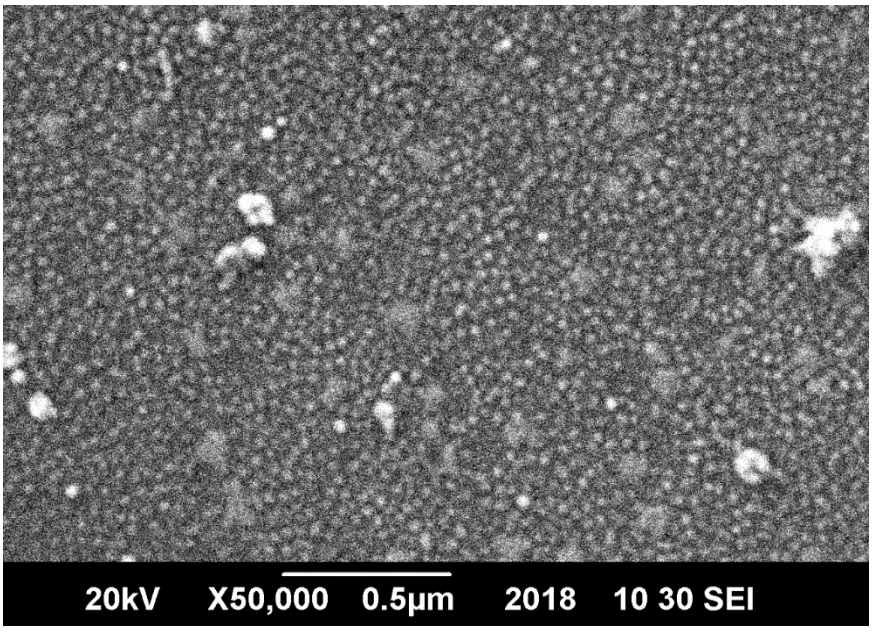

Figure 4.3 SEM image of pure Cobalt ferrite $CoFe_2O_4$

particles distributed in sample while presence of agglomeration is also evident from images in Figure due to this process some of the clusters are formed and agglomeration is because of magnetic nature ,clustering of particles is by weak surface interaction the average size of particle increase with increase concentration of Silver reason for this is the presence of secondary phase. [38]

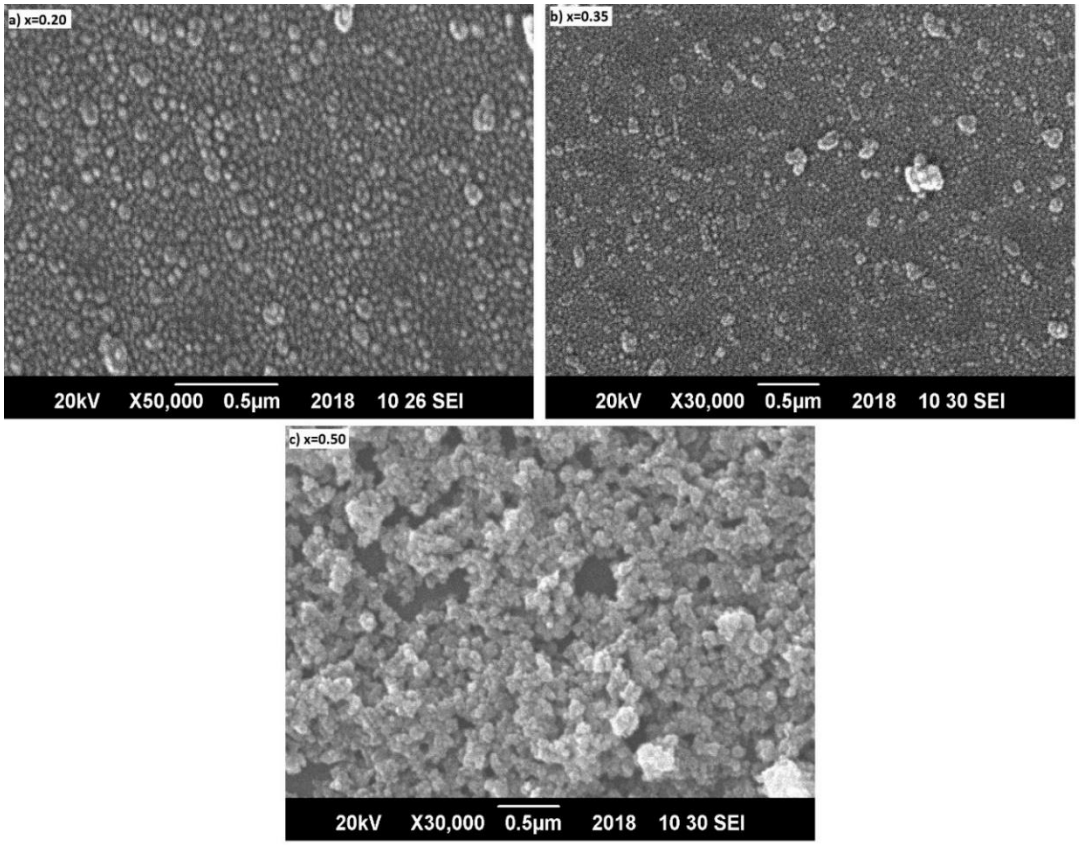

Figure 4.4 SEM images for $Ag_xCo_{1-x}Fe_2O_4$ (a)x=0.20, (b)x=0.35, (c)x=0.50

4.4 Dielectric Constant

The dielectric properties of Cobalt ferrite and loaded cobalt ferrite with copper and silver was measured with the help of LCR meter (WK-6500B). From LCR meter we obtained change in Dielectric constant, Dielectric loss (real permittivity), Tan loss (imaginary permittivity) and A.C conductivity relative to frequency. These plots between frequency and Dielectric constant. It is a theoretical assumption that the dielectric constant decreases as the frequency increases [50]. As the dielectric constant is due to polarization of material and in ferrites the polarization occurs due to exchange of electrons between Fe^{2+} and Fe^{3+} sites. As the frequency increases it decrease the exchange rate of electron between Fe^{2+} and Fe^{3+} ions [47], and after a

certain frequency limit this exchange of electrons stops and decrease the space charge polarization with increased frequency and due to rapid fluctuation in electric field, dipoles do not follow the alternating field and while orienting along field applied, dipoles lags behind, thus after that certain limit or frequency the dielectric remains constant [51] .

In case of sample $Ag_xCo_{1-x}Fe_2O_4$ with x=0.0 which means pure cobalt ferrite, the LCR-meter measured the dielectric constant as 3.62 x 10^{03} at lower frequency and it

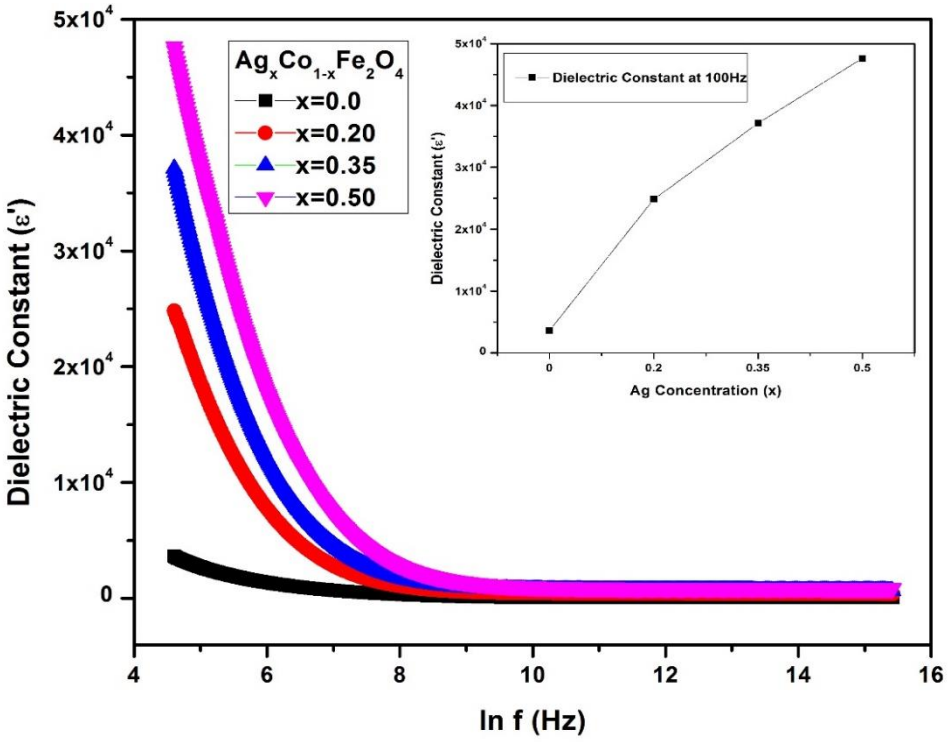

Figure 4.5 Change in Dielectric constant of $Ag_xCo_{1-x}Fe_2O_4$ with respect to frequency

decreases with increase in frequency as per theoretical assumptions and after a certain frequency it became constant [50]. As it is shown in the plot in figure 4.5 that the dielectric constant is increased at lower frequencies as we increase the concentration of silver in it by x=0.20, 0.30 and x=0.50. Due to increase in concentration of Silver which in more conductive the rate of exchange of electrons between Fe^{2+} and Fe^{3+} increases which increases the polarization which is according to Maxwell and Wagner model about space charge polarization [47]. this polarization by dipolar ferrite with conductive metal as silver also play part in storing charge [30]. The dielectric constant measured for $Ag_xCo_{1-x}Fe_2O_4$ increases from 3.62 x 10^{03} at x=0.0 to 4.76 x 10^{04} at x=0.50, As silver offer easier path to electrons to exchange, due its greater

conductivity it has enhanced value of di electric constant. these values are also shown in table 4.2

Table 4.2 Values of Dielectric Constant at 100 Hz for $Ag_xCo_{1-x}Fe_2O_4$

Dielectric Constant (ε′) at 100 Hz	
Sample(x)	**$Ag_xCo_{1-x}Fe_2O_4$**
0.0	**3.62×10^{03}**
0.20	**2.48×10^{04}**
0.35	**3.71×10^{04}**
0.50	**4.76×10^{04}**

4.5 Dielectric Loss

The imaginary permittivity or dielectric loss is associated with energy dissipation also decreases theoretically with increase in frequency and become constant after certain frequency this can be elaborated by the Koop's theory [46] according to this high resistance behavior is due to grain boundaries where hooping electrons require more energy (high energy loss) to hop or exchange between Fe^{+3} and Fe^{+2} ions, at high frequencies there is already enough energy requiring very low for hopping electrons so loss of energy is low at high frequencies. . In the graph similar trends was obtained from our samples.

As in case of $Ag_xCo_{1-x}Fe_2O_4$ the value of imaginary permittivity or di electric loss is equal to 6.52×10^{03} for x=0.0 at 100 Hz and from the graph in the figure 4.6 it is clear that value of imaginary permittivity increases as we increase the concentration of copper in samples due to formation of defects and voids [51]. The values di electric loss for x=0.50 at 100 Hz is 2.06×10^{05} also given in table 4.3 below

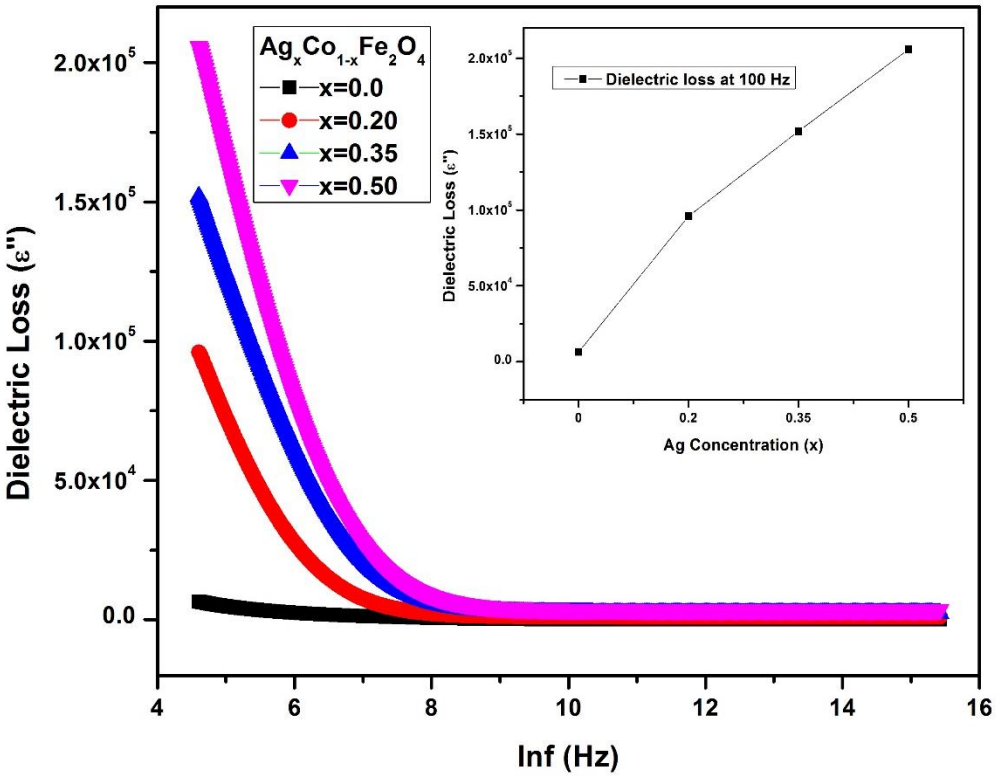

Figure 4.6 Change in Di electric Loss of $Ag_xCo_{1-x}Fe_2O_4$ with respect to frequency

Table 4.3 Values of Dielectric Loss at 100 Hz for $Ag_xCo_{1-x}Fe_2O_4$

Di electric Loss (ε′′) at 100 Hz	
Sample(x)	**$Ag_xCo_{1-x}Fe_2O_4$**
0.0	**6.52×10^{03}**
0.20	**9.60×10^{04}**
0.35	**1.52×10^{05}**
0.50	**2.06×10^{05}**

4.6 Tangent loss Factor

Tangent loss or Di electric tangent loss is in fact the measure of the relative loss of electrical energy which over the frequency encountered by the electrical field which means this loss of relative energy is due to rapid electric field fluctuations [50]. Dielectric loss tangent also showed similar behavior as dielectric constant and dielectric loss. It also decreased with increase in frequency and become constant after a certain value of frequency [51]. We also know that tangent loss is a ratio between di electric loss and di electric constant.

For $Ag_xCo_{1-x}Fe_2O_4$ with increasing concentration of copper from x=0.0 to x=0.5 the value of tangent loss also increases and exhibit dispersion in accordance with the Koop's theory. At low frequency tangent loss is very high due to disruption in passage of electric field when majority charge carriers of dipoles interact with it [47]. While at high frequency it is almost constant or independent of frequency alteration. This is also evident from graph plot in figure 4.7 and values are given in table 4.7

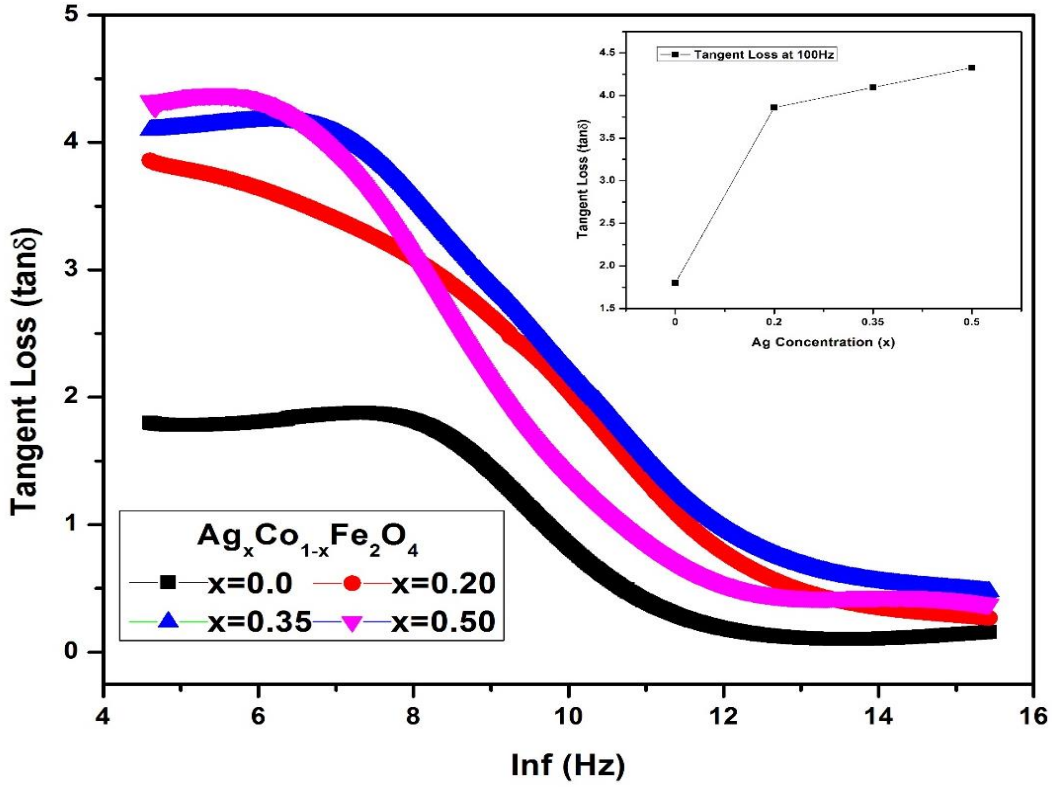

Figure 4.7 Change in Tangent loss factor (tanδ) of $Ag_xCo_{1-x}Fe_2O_4$ with respect to frequency

Table 4.4 Values of Tangent loss factor (tanδ) at 100 Hz for $Ag_xCo_{1-x}Fe_2O_4$

Tan loss factor (tanδ) at 100 Hz	
Sample(x)	**$Ag_xCo_{1-x}Fe_2O_4$**
0.0	**1.80**
0.20	**3.86**
0.35	**4.10**
0.50	**4.33**

4.7 AC Conductivity

AC conductivity in ferrites can be explained by hopping model [52]. The conductive nature provides a specific path for the hopping of electrons between the ions of ferrites and due to which the AC conductivity also increases with increase in content of conductive materials such as Copper and silver. Also, band conduction dominates on hopping at low frequencies while at high frequency this reverses and hopping conduction dominate [50]. This type of behavior is referred to polaron which if are small, increases the Ac conductivity with increasing frequency [44]. Beside the concentration values of Ac conductivity are higher for the Silver, this is because Silver is more conductive than the copper and provide more free electrons along

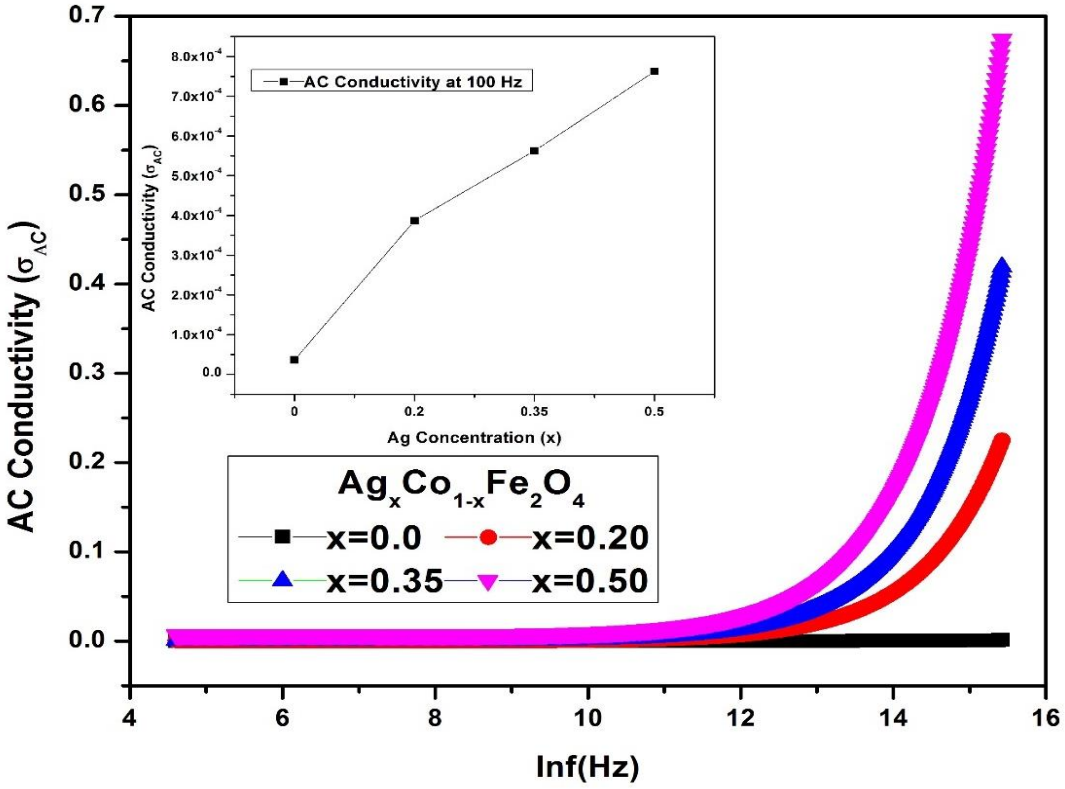

Figure 4.8 Change in Ac Conductivity of $Ag_xCo_{1-x}Fe_2O_4$ with respect to frequency

Table 4.5 Values of Ac Conductivity for $Ag_xCo_{1-x}Fe_2O_4$

Ac conductivity (σ_{AC}) S/m	
Sample(x)	**$Ag_xCo_{1-x}Fe_2O_4$**
0.0	**9.70×10^{-04}**
0.20	**2.25×10^{-01}**
0.35	**4.19×10^{-01}**
0.50	**6.68×10^{-01}**

4.8 Impedance

Impedance was measured by the same LCR-meter used for finding the dielectric properties of our sample and in the same range of frequency. Fig is the plot obtained

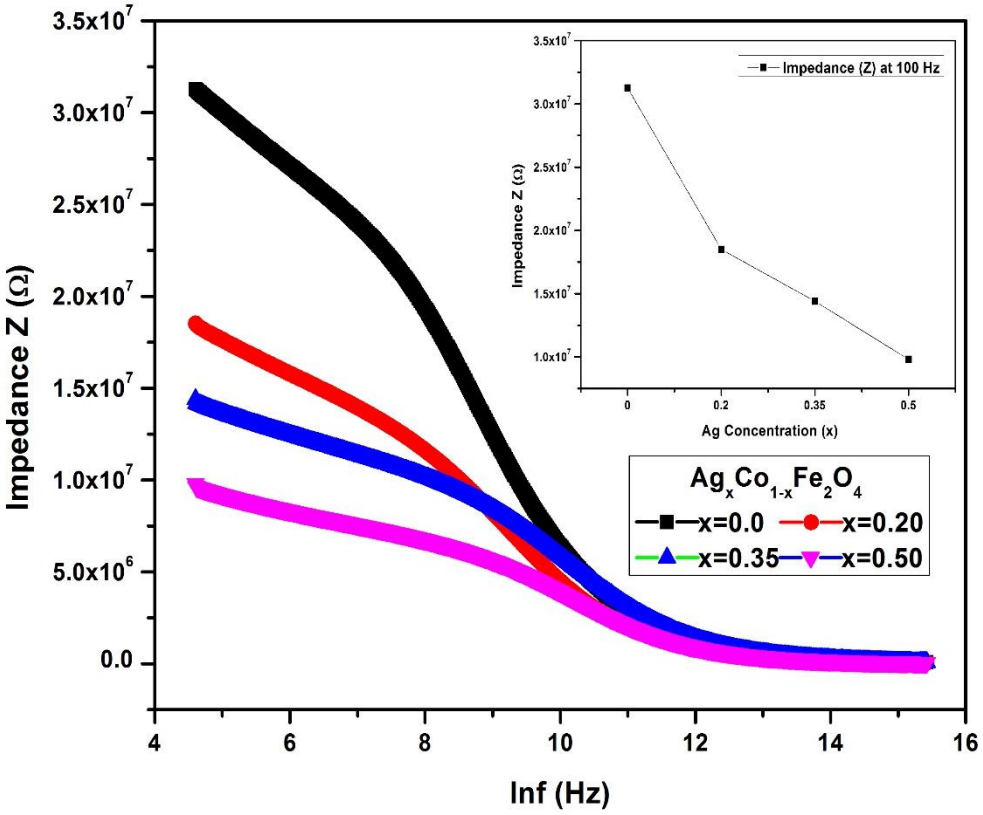

Figure 4.9 Change in Impedance of $Ag_xCo_{1-x}Fe_2O_4$ with respect to frequency

from the data of LCR-meter, which is between the frequency applied and impedance measured. Like other electrical properties the impedance also shows the similar trend which higher at lower frequency and then decreasing with increase in frequency and after that it become constant. As impedance is concerned with the flow of electrons between the Fe^{2+} and Fe^{3+} ions in ferrites. As it is clear from the graph figure 4.9 that impedance decreases as we increase the concentration of silver in $Ag_xCo_{1-x}Fe_2O_4$ where x=0.0, 0.20, 0.35,0.50.as we know cobalt have high resistivity so by the addition of conductive part in it silver provide a specific smooth way for the flow of electrons between the ions of ferrites which decrease the impedance or resistance offered to the flow of electrons [2]. The impedance value for $Ag_xCo_{1-x}Fe_2O_4$ at x=0.0 means pure cobalt ferrite was 3.13×10^{07} Ω which was at 100 Hz decreased to 9.80×10^{06} Ω for x=0.50 . The impedance values for each sample is given in Table 4.6.

Table 4.6 Values of Impedance at 100 Hz for $Ag_xCo_{1-x}Fe_2O_4$

Impedance (Z) at 100Hz Ω	
Sample (x)	**$Ag_xCo_{1-x}Fe_2O_4$**
0.0	**3.13×10^{07}**
0.20	**1.85×10^{07}**
0.35	**1.44×10^{07}**
0.50	**9.80×10^{06}**

The graphs for the real and imaginary part of the impedance are also shown in figure 4.10 and 4.11 respectively along with tables 4.7 and 4.8 of their values for silver loaded samples below.

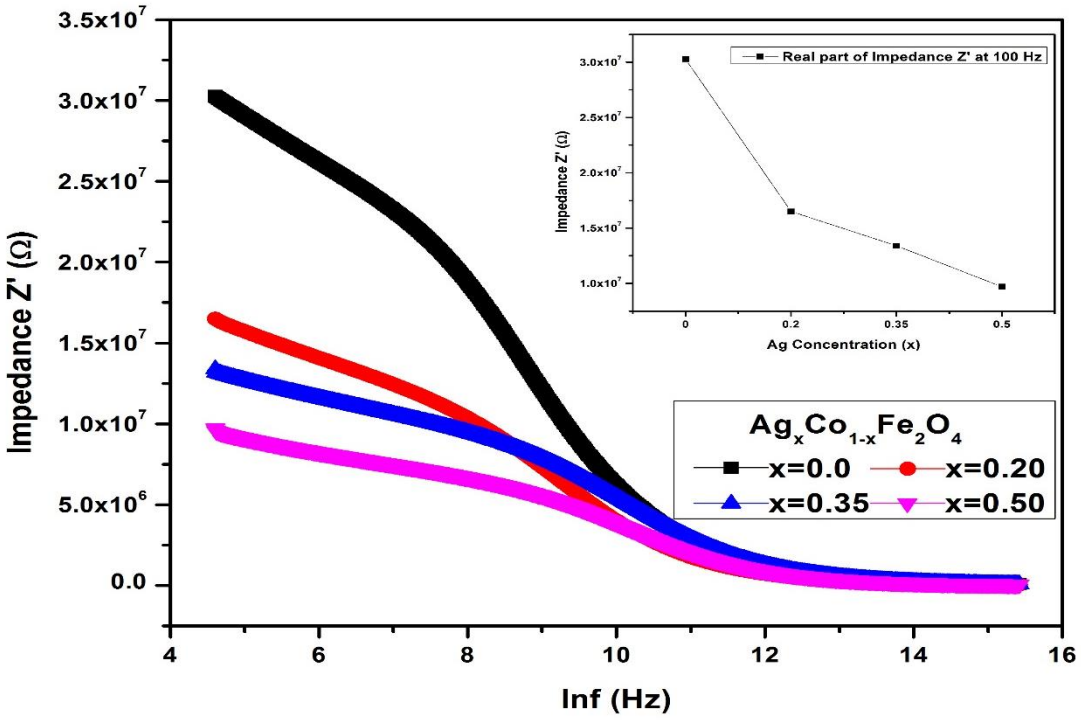

Figure 4.10 Change in real part of Impedance of $Ag_xCo_{1-x}Fe_2O_4$ with respect to frequency

Table 4.7 Values of Real part of Impedance at 100 Hz for $Ag_xCo_{1-x}Fe_2O_4$

Impedance Real (Z′) at 100 Hz Ω	
Sample(x)	**$Ag_xCo_{1-x}Fe_2O_4$**
0.0	**3.03×10^{07}**
0.20	**1.65×10^{07}**
0.35	**1.34×10^{07}**
0.50	**9.70×10^{06}**

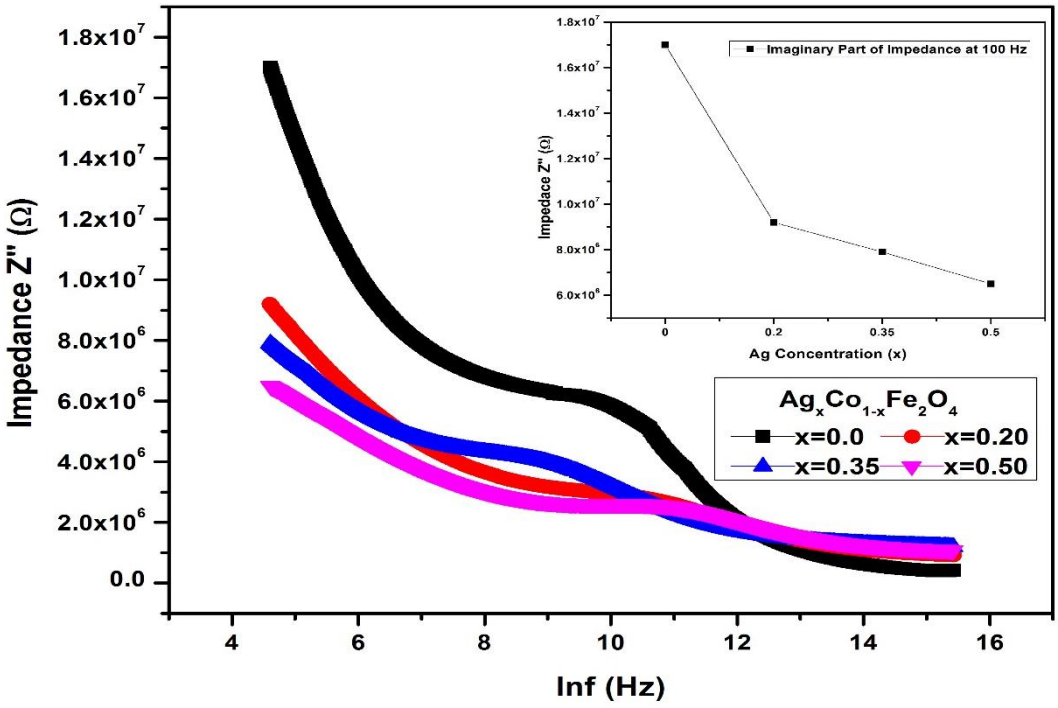

Figure 4.11 Change in imaginary part of Impedance of $Ag_xCo_{1-x}Fe_2O_4$ with respect to frequency

Table 4.8 Values of imaginary part of Impedance at 100 Hz for $Ag_xCo_{1-x}Fe_2O_4$

Impedance Imaginary (Z′′) at 100 Hz Ω	
Sample(x)	**$Ag_xCo_{1-x}Fe_2O_4$**
0.0	**1.70×10^{07}**
0.20	**9.20×10^{06}**
0.35	**7.90×10^{06}**
0.50	**6.50×10^{06}**

Figure 4.12 shows a cole-cole plot between real and imaginary portions of Impedance This gives us the contribution grain boundary distribution in the resistance of material, from plot it's clear that grains contributed resistance is not resolved very well [50]. We can get information about homogeneity conductive and dielectric properties from semi-circle of cole-cole plot [51]. Magnitude of the resistance in cole-cole plot is demonstrated by the size of the semi-circle we can easily observe that with increase on concentration of silver it decreases, the grain boundary resistance of sample x=0.50 is smallest while x=0.0 shows greater resistance for silver. Smaller value of grain boundary resistance provides us information that charge transfer and electron hole pair separation is efficient in x=0.50 while more efficient in $Ag_xCo_{1-x}Fe_2O_4$ at x=0.50 with it electron hopping also increases.

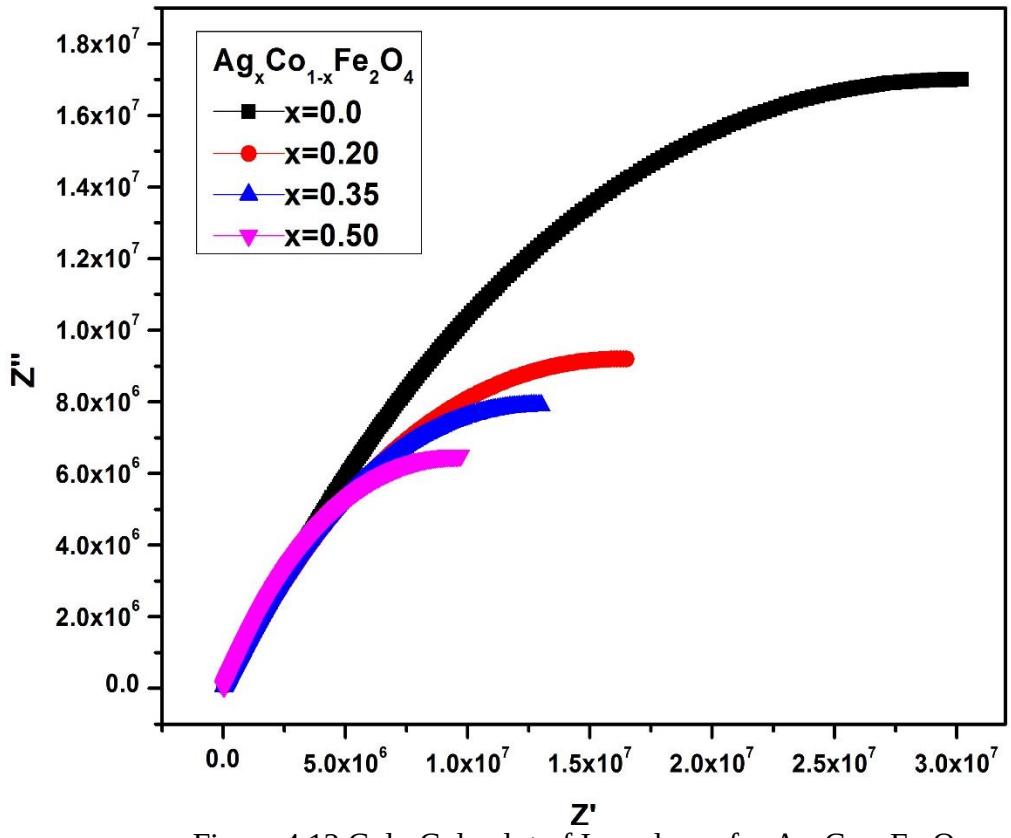

Figure 4.12 Cole-Cole plot of Impedance for $Ag_xCo_{1-x}Fe_2O_4$

4.9 DC Resistivity

DC resistivity is measured for $Ag_xCo_{1-x}Fe_2O_4$ with different concentration (x) as a function of temperature. The plots for the measured DC resistivity is shown in figure 4.13. The plots show a gradual decrease in the resistivity with increase in temperature [53]. By increase in temperature the electrons get more energy and which the conduction of electrons across the sample easier and hence its resistivity decreases at higher temperature [45]. The DC resistivity decreased as we increased concentration (x) of silver. By increase in x (concentration silver) the Dc resistivity decreases due to the electrical properties and conductive nature of these metals. The DC resistivity was measured from temperature (T) and Current (I) values at constant voltage(V).

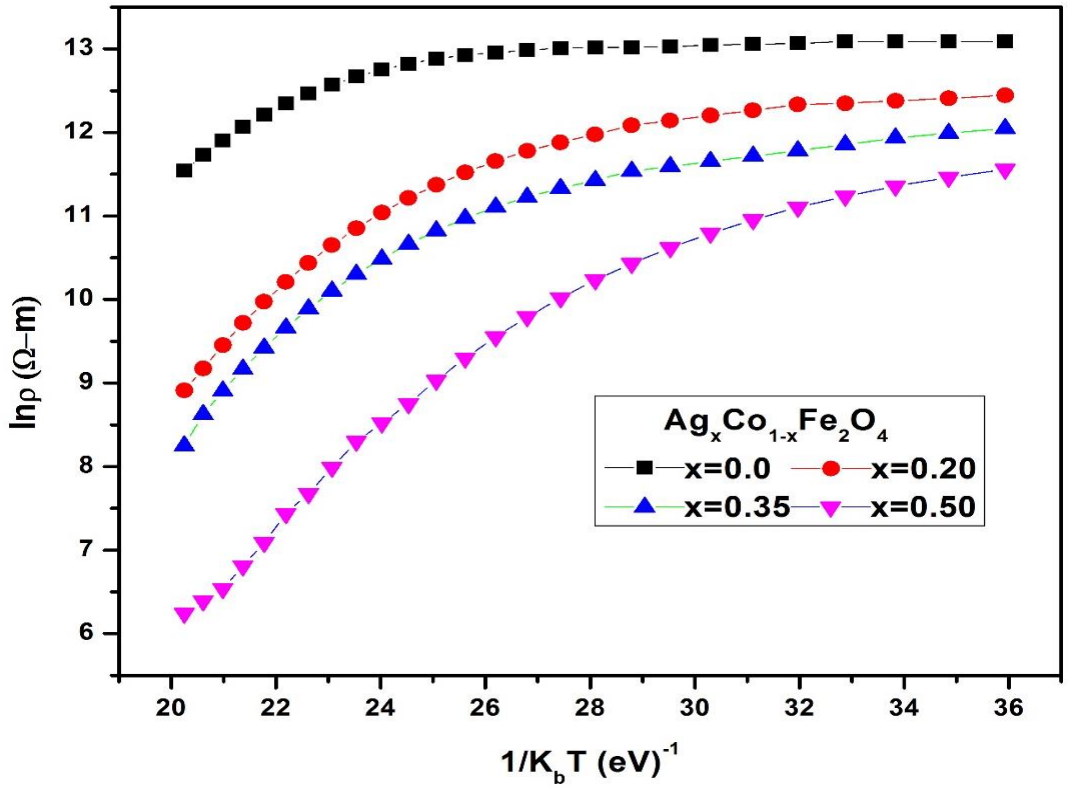

Figure 4.13 Change in DC Resistivity with $1/k_bT$ or temperature for $Ag_xCo_{1-x}Fe_2O_4$

Table 4.9 Values of DC resistivity at 373K for $Ag_xCo_{1-x}Fe_2O_4$

DC Resistivity Ω-m at 373 K	
Sample(x)	**$Ag_xCo_{1-x}Fe_2O_4$**
0.0	**4.68×10^{05}**
0.20	**2.12×10^{05}**
0.35	**1.22×10^{05}**
0.50	**5.72×10^{04}**

4.10 Electric Modulus

Electric modulus is a very useful phenomenon by which one can characterize the conduction and relaxation behavior of ionic and conducting ceramic materials. The complex electric modulus is also defined as the inverse of complex relative permittivity [50]. Figure 4.14 and 4.15 shows the behavior of real and imaginary part of Electric modulus with respect to frequency. Where figure 4.16 shows the graph between Real part of Electric modulus (M') and imaginary part of electric modulus (M'') which is also known as Cole-Cole diagram. The real and imaginary part of electric modulus was calculated by the help of following equations

$$Real\ part:\ M' = \frac{\varepsilon'}{\varepsilon'^2 + \varepsilon''^2}$$

$$Imaginary\ part: M'' = \frac{\varepsilon''}{\varepsilon'^2 + \varepsilon''^2}$$

As we discussed that the electric modulus or complex electric modulus shows the conduction and relaxation behavior [51], as from Fig 4.14 the real part of electric modulus increases as we increase the concentration of metals x in $Ag_xCo_{1-x}Fe_2O_4$. The increase in the electric modulus indicates the increase in the conductivity of our samples due to increase content.

Fig 4.15 shows the behavior of imaginary part of electric modulus with respect to frequency. In that graph, the dielectric response of our samples against variation in frequency is represented in the form curves or arcs. In this figure, the maximum values of curve or arcs are shifted towards the higher frequency as we increase the concentration of metals in cobalt ferrite. This change in the imaginary part of electric modulus shows the relaxation rate, the relaxation rate is decreases as the peaks are shifted towards the high frequency range [50]. The values for imaginary part of electric modulus (M") in the start remain constant then increases with increase in frequency i.e. the dipole oscillated frequency increases with applied frequency and then at a certain value where the oscillating frequency matches the applied frequency give us a maximum on the graph and known as relaxation frequency. After the relaxation frequency is achieved the graph is shifted toward the lower values of M" due to increase in grain boundaries contribution to resistance.

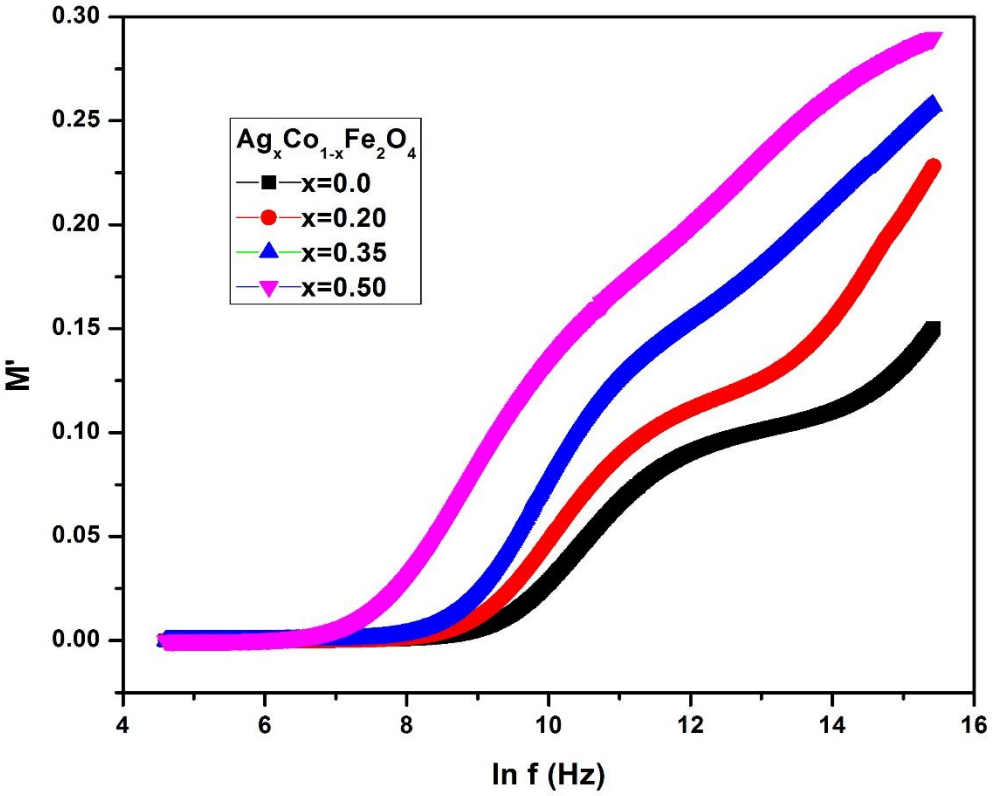

Figure 4.14 Change in Real part of Electric Modulus (M′) with frequency for $Ag_xCo_{1-x}Fe_2O_4$

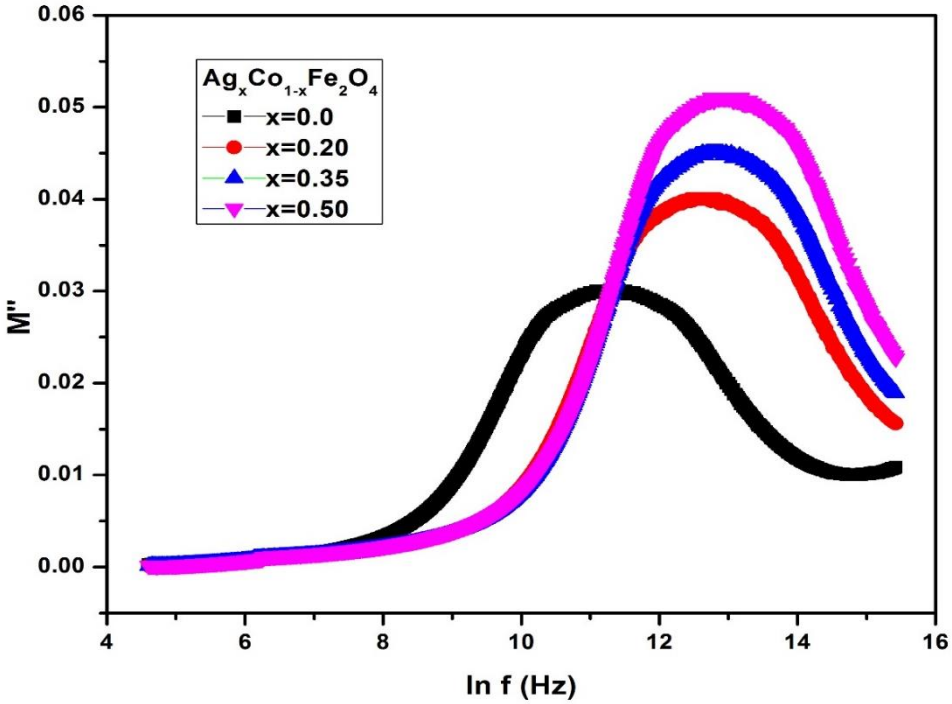

Figure 4.15 Change in imaginary part of Electric Modulus (M″) with frequency for $Ag_xCo_{1-x}Fe_2O_4$

Fig 4.16 shows the graph between real and imaginary part of Electric modulus i.e. M' vs M", this graph is also known as Cole-Cole diagram. It is obvious from graph that the maximum of the arcs shifted toward the higher values of M' as we increase the content of metals in Cobalt ferrite. This behavior shows that the relaxation rate is decreases and the conduction of the electrons increases which in result increases the conductance of our sample. Thus, the increase in the concentration x in the $Ag_xCo_{1-x}Fe_2O_4$ make the material more conductive and increase the dielectric loss.

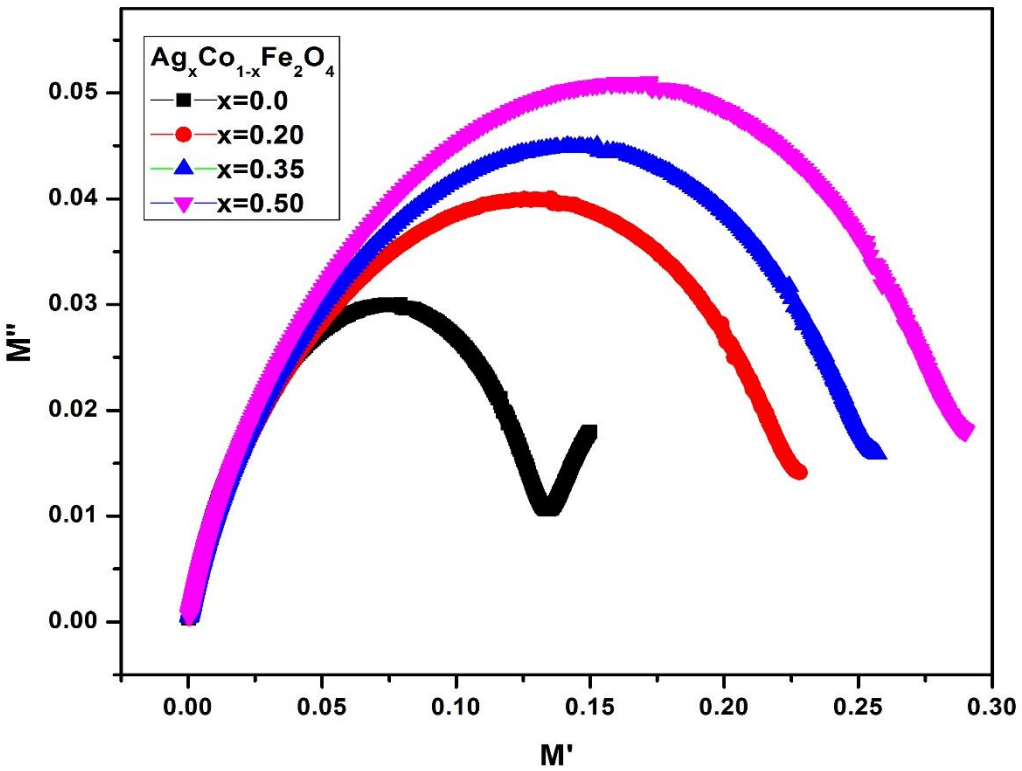

Figure 4.16 Cole-Cole plot of Electric Modulus for $Ag_xCo_{1-x}Fe_2O_4$

4.11 Summary

Summarized values of data of Dielectric properties and electrical properties silver loaded $Ag_xCo_{1-x}Fe_2O_4$ are here separately given below in tabular form in

Table 4.10 Summary of data values of properties of $Ag_xCo_{1-x}Fe_2O_4$ at different concentrations (x)

$Ag_xCo_{1-x}Fe_2O_4$				
Sample (x)	**0.0**	**0.20**	**0.35**	**0.50**
Di electric Constant (ε′)	**3.62×10^{03}**	**2.48×10^{04}**	**3.71×10^{04}**	**4.76×10^{04}**
Di electric Loss (ε′′)	**6.52×10^{03}**	**9.60×10^{04}**	**1.52×10^{05}**	**2.06×10^{05}**
Tan Loss (tanδ)	**1.80**	**3.86**	**4.10**	**4.33**
Impedance (Z) Ω	**3.13×10^{07}**	**1.85×10^{07}**	**1.44×10^{07}**	**9.80×10^{06}**
Imaginary Z	**1.70×10^{07}**	**9.20×10^{06}**	**7.90×10^{06}**	**6.50×10^{06}**
Real Z	**3.03×10^{07}**	**1.65×10^{07}**	**1.34×10^{07}**	**9.70×10^{06}**
Ac conductivity(σ_{AC}) S/m at max frequency	**9.70×10^{-04}**	**2.25×10^{-01}**	**4.19×10^{-01}**	**6.68×10^{-01}**
Ac conductivity(σ_{AC}) S/m at 100 Hz	**3.63×10^{-05}**	**3.87×10^{-04}**	**5.63×10^{-04}**	**7.62×10^{-04}**
DC resistivity (Ω-m) lnρ At 373 K	**13.056**	**12.265**	**11.715**	**10.954**

4.12 Conclusions

- Cobalt ferrite was conveniently synthesized and afterward loaded with silver via wet chemical co-precipitation route and it was confirmed with the help of X ray diffraction that it is Cobalt ferrite and silver in accordance with JCPDS, spinel cubic crystal structure was confirmed with FTIR.
- It is clear from data in Summary that Average Crystallite Size for silver loaded was 31- 44 nm
- In accordance with literature the dielectric constant of all samples decreased with increasing in frequency and then after a certain point it became constant.
- The dielectric constant clearly enhanced from 3.62 x 10^{03} to 4.76 x 10^{04} by increasing the concentration of Silver from x =0.0 to x=0.50 $Ag_xCo_{1-x}Fe_2O_4$.
- Similar to dielectric constant, Dielectric loss also increases form 6.52 x 10^{03} to 2.06 x 10^{05} with for silver. Tangent Loss, Impedance, Ac conductivity got enhanced with increasing concentration of conductive metal in cobalt ferrite whose values are given in Summary.
- Cobalt ferrite with silver synthesized with enhanced electrical or dielectric properties, silver offered more enhanced properties.

4.13 Future perspective

In future magnetic properties of these samples will studied

- Try to synthesize them with different chemical routes to improve quality and yield to make it cost effective.
- Study their application in microwave absorption and EMI shielding also try its biomedical application as silver and copper are very promising medical materials.

References

[1] R. Srivastava and B. C. Yadav, “Ferrite Materials: Introduction, Synthesis Techniques, and Applications as Sensors,” *Int. J. Green Nanotechnol.*, vol. 4, no. 2, pp. 141–154, Apr. 2012.

[2] W. Callister and D. Rethwisch, *Materials science and engineering: an introduction*, vol. 94. 2007.

[3] R. Valenzuela, “Novel applications of ferrites,” *Phys. Res. Int.*, vol. 2012, 2012.

[4] T. Indira, “Magnetic Nanoparticles: A Review,” *Int. J. Pharm.*, vol. 3, no. 3, pp. 1035–1042, 2010.

[5] J. M. D. Coey, *Magnetism and Magnetic Materials*, vol. 46, no. 1–2. Cambridge: Cambridge University Press, 2010.

[6] W. H. Bragg, “XXX. The structure of the spinel group of crystals,” *London, Edinburgh, Dublin Philos. Mag. J. Sci.*, vol. 30, no. 176, pp. 305–315, 1915.

[7] D. S. Mathew and R. S. Juang, “An overview of the structure and magnetism of spinel ferrite nanoparticles and their synthesis in microemulsions,” *Chem. Eng. J.*, vol. 129, no. 1–3, pp. 51–65, 2007.

[8] A. Eloizo, A. F. de Siqueira, C. Silva Danna, F. Silva, F. Camargo, and L. E. Kerche, “Utilization of Composites and Nanocomposites Based on Natural Rubber and Ceramic Nanoparticles as Control Agents for Leishmania braziliensis,” in *Leishmaniasis - Trends in Epidemiology, Diagnosis and Treatment*, InTech, 2014.

[9] H. B. G. Casimir *et al.*, “Rapport sur quelques recherches dans le domaine du magnétisme aux laboratoires Philips,” *J. Phys. le Radium*, vol. 20, no. 2–3, pp. 360–373, 1959.

[10] H. Kumar, R. C. Srivastava, P. Negi, H. M. Agrawal, and K. Asokan, “Dielectric Behaviour of Cobalt Ferrite Nanoparticles,” vol. 2, no. 1, pp. 59–66, 2013.

[11] S. Sumathi and V. Lakshmipriya, “Structural, magnetic, electrical and

catalytic activity of copper and bismuth co-substituted cobalt ferrite nanoparticles," *J. Mater. Sci. Mater. Electron.*, vol. 28, no. 3, pp. 2795–2802, 2017.

[12] M. krishna Surendra, "Magnetic and dielectric properties study of cobalt ferrite nanoparticles synthesized by co-precipitation method," *Mater. Res. Soc.*, vol. 1368, no. 5, pp. 1001–1006, 2011.

[13] C. Murugesan, M. Perumal, and G. Chandrasekaran, "Structural, dielectric and magnetic properties of cobalt ferrite prepared using auto combustion and ceramic route," *Phys. B Condens. Matter*, vol. 448, pp. 53–56, 2014.

[14] A. K. Gurjas Kaur, Tanvir Singh, "Nanotechnology: a review.," *J. Pharm. Res.*, vol. 2, no. 1, pp. 50–53, 2012.

[15] K. Maaz, A. Mumtaz, S. K. Hasanain, and A. Ceylan, "Synthesis and magnetic properties of cobalt ferrite (CoFe2O4) nanoparticles prepared by wet chemical route," *J. Magn. Magn. Mater.*, vol. 308, no. 2, pp. 289–295, 2007.

[16] N. Ponpandian, P. Balaya, and A. Narayanasamy, "Electrical conductivity and dielectric behaviour of nanocrystalline NiFe 2 O 4 spinel," *J. Phys. Condens. Matter*, vol. 14, no. 12, pp. 3221–3237, Apr. 2002.

[17] A. Sihvola, "Dielectric polarization and particle shape effects," *J. Nanomater.*, vol. 2007, no. December, 2007.

[18] F. E. Harris and S. G. Brush, "Dipole Moments and Dielectric Polarization in Solutions," *J. Am. Chem. Soc.*, vol. 78, no. 7, pp. 1280–1287, 1956.

[19] M. Savinov *et al.*, "Dielectric and polarization studies of magnetoelectric coupling in non-relaxor Pb(Fe1/2Ta1/2)O3multiferroic ceramics," *Ferroelectrics*, vol. 509, no. 1, pp. 80–91, 2017.

[20] T. Toyoda, S. Sasaki, and M. Tanaka, "Evidence of charge ordering of Fe2+ and Fe3+ in magnetite observed by synchrotron X-ray anomalous scattering," *Am. Mineral.*, vol. 84, no. 3, pp. 294–298, 1999.

[21] M. Jackson, B. Moskowitz, and J. Bowles, "The magnetite Verwey transition," *IRM Q.*, vol. 20, no. 4, pp. 1–11, 2011.

[22] M. Naeem Ashiq, A. Sami Asi, S. Farooq, M. Najam-ul-Haq, and S. Rehman, "Magnetic and electrical properties of M-type nano-strontium hexaferrite prepared by sol-gel combustion method," *J. Magn. Magn. Mater.*, vol. 444, no. October, pp. 426–431, 2017.

[23] R. M. Almeida, W. Paraguassu, D. S. Pires, R. R. Corrêa, and C. W. de Araujo Paschoal, "Impedance spectroscopy analysis of BaFe12O19M-type hexaferrite obtained by ceramic method," *Ceram. Int.*, vol. 35, no. 6, pp. 2443–2447, 2009.

[24] S. H. Mahmood, A. M. Awadallah, I. Bsoul, and Y. Maswadeh, "Structural and magnetic properties of lightly doped M-type hexaferrites," pp. 1–20, 2017.

[25] W. M. Samuel J. Ling, Eff Sanny, *University Physics Volume 2*. OpenStax. Rice Universit, 2016.

[26] K. Sinkó, E. Manek, A. Meiszterics, K. Havancsák, U. Vainio, and H. Peterlik, "Liquid-phase syntheses of cobalt ferrite nanoparticles," *J. Nanoparticle Res.*, vol. 14, no. 6, 2012.

[27] M. Easwari, A. Kalaivani, A. C. Joy, and S. Jesurani, "Synthesis and properties of cobalt ferrite magnetic nanoparticles," vol. 14, no. 1, 2014.

[28] K. B. S. Sathiya, K. Parasuraman, M. Anbarasu, "FT-IR , XRD and SEM Study of MnFe 2 O 4 Nanoparticles by Chemical Co-precipitation Method," *Int. Res. J. Nano Sci. Technol.*, vol. 5, no. 4, pp. 63–68, 2015.

[29] D. Sophia, M. Ragam, and S. Arumugam, "Synthesis and Characterisations of Cobalt Ferrite Nanoparticles," *Int. J. Sci. Res. Mod. Educ.*, pp. 2455–5630, 2016.

[30] M. Kurian *et al.*, "Structural, magnetic, and acidic properties of cobalt ferrite nanoparticles synthesised by wet chemical methods," *J. Adv. Ceram.*, vol. 4, no. 3, pp. 199–205, 2015.

[31] S. Jovanovi, M. Spreitzer, M. Otoni, and D. Suvorov, "Synthesis of cobalt ferrite nanoparticles using a combination of the co-precipitation and hydrothermal methods," vol. 71, no. 12, p. 7509, 2008.

[32] K. Khan, “Microwave absorption properties of radar absorbing nanosized cobalt ferrites for high frequency applications,” *J. Supercond. Nov. Magn.*, vol. 27, no. 2, pp. 453–461, 2014.

[33] G. B. Alcantara, L. G. Paterno, F. J. Fonseca, M. A. Pereira-Da-Silva, P. C. Morais, and M. A. G. Soler, “Dielectric properties of cobalt ferrite nanoparticles in ultrathin nanocomposite films,” *Phys. Chem. Chem. Phys.*, vol. 15, no. 45, pp. 19853–19861, 2013.

[34] N. Sivakumar, A. Narayanasamy, C. N. Chinnasamy, and B. Jeyadevan, “Influence of thermal annealing on the dielectric properties and electrical relaxation behaviour in nanostructured CoFe $_2$ O $_4$ ferrite,” *J. Phys. Condens. Matter*, vol. 19, no. 38, p. 386201, 2007.

[35] G. P. Sandhya Singh, Gaurav Hitkari, “Synthesis, Characterization of Fe3O4, CoFe2O4 Nanomaterials and its Application in Photodegradation of Rhodamin B dye,” vol. 56, no. 5, pp. 299–311, Dec. 2017.

[36] Shinde. A .B, “Structural and Electrical Properties of Cobalt Ferrite Nanoparticles,” *Int. J. Innov. Technol. Explor. Eng.*, vol. 3, no. 4, pp. 64–67, 2013.

[37] R. k. Singh, “Synthesis and Characterization of Cobalt Ferrite Nanoparticles,” *Raghavender AT*, vol. 7522, no. 4, pp. 1–4, 2013.

[38] J. Balavijayalakshmi, N. Suriyanarayanan, and R. Jayapraksah, “Influence of copper on the magnetic properties of cobalt ferrite nano particles,” *Mater. Lett.*, vol. 81, pp. 52–54, 2012.

[39] S. Xavier, H. Cleetus, N. Pj, S. Thankachan, R. M. Sebastian, and M. Em, “Research Journal of Pharmaceutical , Biological and Chemical Sciences Structural and Antibacterial Properties of Silver Substituted Cobalt Ferrite September - October,” *Res. J. Pharm. Biol. Chem. Sci.*, vol. 5, no. 364, pp. 179–186, 2014.

[40] “Coprecipitation - Wikipedia.” [Online]. Available: https://en.wikipedia.org/wiki/Coprecipitation.

[41] I. M. Kolthoff, “Theory of coprecipitation,” no. I, pp. 407–409, 1932.

[42] I. H. Gul, A. Z. Abbasi, F. Amin, M. Anis-ur-Rehman, and A. Maqsood, "Structural, magnetic and electrical properties of Co1-xZnxFe2O4synthesized by co-precipitation method," *J. Magn. Magn. Mater.*, vol. 311, no. 2, pp. 494–499, 2007.

[43] B. D. Cullity, *Elements of X-Ray Diffraction*, Pearson ne. 2010.

[44] B. Hafner and B. Hafner, "Scanning Electron Microscopy Primer," *Cities*, pp. 1–29, 2007.

[45] J. S. Gaffney, N. A. Marley, and D. E. Jones, "Fourier Transform Infrared (FTIR) Spectroscopy," *Charact. Mater.*, 2012.

[46] "Michelson-Morley Experiment -- from Eric Weisstein's World of Physics." [Online]. Available: http://scienceworld.wolfram.com/physics/Michelson-MorleyExperiment.html.

[47] Ž. Cvejić, S. Rakić, S. Jankov, S. Skuban, and A. Kapor, "Dielectric Properties of Nanosized ZnFe2O4," *Process. Appl. Ceram.*, vol. 2, no. 1, pp. 53–56, 2008.

[48] R. S. Totagi, R. B. Pujar, and S. B. Koujalagi, "Synthesis, characterization, study of electrical properties and survey of applications of nanoferrites-an approach by chemical method," vol. 6, no. 3, pp. 272–279, 2014.

[49] M. Shen, S. Ge, and W. Cao, "Dielectric enhancement and Maxwell-Wagner effects in polycrystalline ferroelectric multilayered thin films," *J. Phys. D. Appl. Phys.*, vol. 34, no. 19, pp. 2935–2938, 2001.

[50] A. Samavati and A. F. Ismail, "Antibacterial properties of copper-substituted cobalt ferrite nanoparticles synthesized by co-precipitation method," *Particuology*, vol. 30, pp. 158–163, 2017.

[51] A. R. Denton and N. W. Ashcroft, "Vegard's law," *Phys. Rev. A*, vol. 43, no. 6, pp. 3161–3164, Mar. 1991.

[52] C. E. Ciomaga *et al.*, "Preparation and magnetoelectric properties of NiFe 2O 4-PZT composites obtained in-situ by gel-combustion method," *J. Eur. Ceram. Soc.*, vol. 32, no. 12, pp. 3325–3337, 2012.

[53] I. H. Gul and E. Pervaiz, “Comparative study of NiFe2-xAlxO4ferrite nanoparticles synthesized by chemical co-precipitation and sol-gel combustion techniques,” *Mater. Res. Bull.*, vol. 47, no. 6, pp. 1353–1361, 2012.

[54] T. T. N. Vu, G. Teyssedre, S. Le Roy, and C. Laurent, “Maxwell–Wagner Effect in Multi-Layered Dielectrics: Interfacial Charge Measurement and Modelling,” *Technologies*, vol. 5, no. 2, p. 27, 2017.

[55] M. Ajmal and A. Maqsood, “Structural, electrical and magnetic properties of Cu1-xZnxFe2O4ferrites ($0 \leq x \leq 1$),” *J. Alloys Compd.*, vol. 460, no. 1–2, pp. 54–59, 2008.

[56] O. F. Odio and E. Reguera, “Nanostructured Spinel Ferrites: Synthesis, Functionalization, Nanomagnetism and Environmental Applications,” in *Magnetic Spinels - Synthesis, Properties and Applications*, InTech, 2017.

[57] “Top-down and bottom-up processing | Download Scientific Diagram.” [Online]. Available: https://www.researchgate.net/figure/Top-down-and-bottom-up-processing_fig2_289498264.

[58] A. G. Marangoni and M. F. Peyronel, “X-Ray Powder Diffractometry,” Mar. 2013.

[59] “Schematic diagram of SEM 1 | Download Scientific Diagram.” [Online]. Available: https://www.researchgate.net/figure/Schematic-diagram-of-SEM-1_fig3_23567235.